https://doi.org/10.5194/hess-2023-191
Preprint. Discussion started: 31 August 2023

Hydrology and Earth System Sciences
Discussions

How does a warm and low-snow winter impact the snow cover dynamics in a humid and discontinuous boreal forest? An observational study in eastern Canada

Benjamin Bouchard[1,2,5], Daniel F. Nadeau[1,2], Florent Domine[3,4,5], François Anctil[1,2], Tobias Jonas[6], Étienne Tremblay[1]

[1]Department of Civil and Water Engineering, Université Laval, Quebec City, G1V 0A6, Canada
[2]CentrEau – Water Research Centre, Université Laval, Quebec City, G1V 0A6, Canada
[3]Takuvik Joint International Laboratory, Université Laval (Canada) and CNRS-INSU (France), Quebec City, G1V 0A6, Canada
[4]Department of Chemistry, Université Laval, Quebec City, G1V 0A6, Canada
[5]Centre d'Études Nordiques, Université Laval Quebec City, G1V 0A6
[6] WSL Institute for Snow and Avalanche Research (SLF), 7260 Davos Dorf, Switzerland

Correspondence to: Benjamin Bouchard (benjamin.bouchard.1@ulaval.ca)

Abstract. In the boreal forest, winter temperatures are projected to increase substantially by 2100, resulting in a reduction in snow cover thickness and duration. These changes are likely to affect hydrological processes such as snowmelt, the soil thermal regime, and snow metamorphism. The exact impact of future changes is difficult to pinpoint in the boreal forest, due to its complex structure, and the fact that snow dynamics under the canopy are very different from those in the gaps. Although the effects of warmer winters on snow-related processes are well documented, their interactions to influence the spring runoff in evergreen forest remain poorly understood. In this observational study, we assess the influence of a low-snow and warm winter on snowmelt dynamics, soil freezing, snowpack properties, and spring streamflow in a humid and discontinuous boreal catchment of eastern Canada (47.29° N, 71.17° W, ≈ 850 m ASL). We monitored the soil and snow thermal regimes and sampled physical properties of the snowpack under the canopy and in two forest gaps during an exceptionally low-snow and warm winter, plausibly representative of future winters, and during a winter with conditions close to normal. We observe that snowmelt was earlier but slower, top soil layers were cooler, and gradient metamorphism was enhanced during the low-snow and warm winter. However, we observe that snowmelt duration increased in forest gaps, that soil freezing was enhanced only under the canopy, and that snow permeability increased more strongly under the canopy than in either gap. Overall, we observe that the spring streamflow discharge was significantly reduced in the warmest year due to a slower melt and low precipitation in April and May. Our results, based solely on field observations, highlight the complex effects of warmer winters on snow hydrology in discontinuous boreal forests.

https://doi.org/10.5194/hess-2023-191
Preprint. Discussion started: 31 August 2023

Hydrology and Earth System Sciences
Discussions

1 Introduction

The boreal forest is one of the most extensive biomes on Earth. It is projected to warm by up to 5°C by 2100, with the largest increases occurring in winter (Scheffer et al., 2012; Zheng et al., 2023; Price et al., 2013; IPCC, 2022). Warmer winters will result in less solid precipitation and in a thinner, shorter-lived snow cover (Laternser and Schneebeli, 2003; Hamlet et al., 2005). Spring melt will occur earlier in the season, but at a slower rate because less radiative energy is available at that time (López-Moreno et al., 2013; Musselman et al., 2017). Together, these changes are expected to reduce peak spring streamflow and runoff volumes (Furey et al., 2012; Berghuijs et al., 2014; Luce and Holden, 2009; Barnhart et al., 2016). To date, most studies focusing on hydrological changes associated with warmer winters in the boreal forest have looked at rather dry regions of the biome, in western Canada and Europe (Ireson et al., 2015; Shook and Pomeroy, 2012; Xu and Halldin, 1997). The limited number of studies on the humid boreal forest of eastern Canada point towards an increase in mean annual streamflow, but a decrease in snow accumulation and an earlier spring freshet (Guay et al., 2015; Ouranos and MELCCFP, 2022; Valencia Giraldo et al., 2023).

The magnitude of the expected hydrological changes in response to warmer winters depends on a number of processes that occur in the soil–snow–forest–atmosphere continuum. One such process is soil freezing. In forests, the spatial pattern of soil freezing is difficult to determine because snow depth is highly variable and freezing depth and snowpack thickness are inversely proportional (Goodrich, 1982; Zhang, 2005; Hardy et al., 2001). Therefore, it is challenging to understand and predict infiltration versus surface runoff in forested environments during winter. Moreover, the heterogeneity of forested soil freezing is increased by the abundance of macropores (Beven and Germann, 2013). On the one hand, macropores initially rich in air create preferential pathways for infiltration (Granger et al., 1984; Stähli et al., 1996; Fuss et al., 2016). On the other hand, macropores that are rich in ice, for example following a refreeze (Kane and Stein, 1983; Demand et al., 2019), significantly reduce further infiltration (Mohammed et al., 2018; Watanabe and Kugisaki, 2017). Previous studies have reported that both canopy interception, which limits snowpack thickening, and meteorological conditions such as rain-on-snow events followed by a cold spell, which favor water refreezing within macropores, promote runoff over infiltration (Proulx and Stein, 1997; Jones and Pomeroy, 17-19 May 2001; Stadler et al., 1996; Shanley and Chalmers, 1999). With the projected warmer climate leading to more frequent and intense winter rainfalls (Il Jeong and Sushama, 2018), it is therefore important to deepen our understanding of soil freezing dynamics in discontinuous boreal forests.

Forest structure affects not only the dynamics of soil freezing, but also the physical properties of the snowpack. As canopy interception limits snow accumulation under trees (Pomeroy et al., 1998; Mazzotti et al., 2019; Sun et al., 2018), stronger vertical temperature gradients ($\partial T/\partial z$) favor kinetic snow grain growth under the canopy more than in gaps (Albert and Hardy, 8-10 June 1993; Molotch et al., 2016; Bouchard et al., 2022). Bouchard et al. (2022) showed that the phenomenon results in lower specific surface area (SSA) and greater snowpack permeability under the canopy. With warmer winters, one may expect snow surface temperature to increase, but snow thickness to decrease. Domine et al. (2007) have suggested a decrease in permeability with climate warming due to a warmer snow surface, lower $\partial T/\partial z$, and slower grain growth. The authors also

https://doi.org/10.5194/hess-2023-191
Preprint. Discussion started: 31 August 2023


Hydrology and Earth System Sciences
Discussions

noted that an increase in the frequency of melting events would result in more melt-freeze crusts and low-permeability ice layers (Albert and Perron, 2000). In the boreal forest, where snow surface temperature and snow accumulation are highly variable in space (Malle et al., 2019; Parajuli et al., 2020; Mazzotti et al., 2023) and where the canopy structure influences crust formation in the snowpack (Bründl et al., 1999; Teich et al., 2019; Bouchard et al., 2022), the impacts of warmer winters on snow properties may be hard to predict. Therefore, dedicated studies on the influence of warmer winters on snowpack physical properties in discontinuous boreal forests are needed.

Based on the research gaps identified above, we defined two objectives in this study. The first one is to quantify the effect of a low-snow and warm winter on snowmelt, soil freezing and snowpack physical properties in a humid and discontinuous boreal forest. The second one is to evaluate how these factors interact together to modulate spring runoff. To assess this, we compared snow melt, snow physical properties, soil freezing, and spring runoff at a small catchment in the humid boreal forest of eastern Canada, for two consecutive winters. One winter was exceptionally warm and dry, while the other was slightly colder, with precipitation amounts similar to the standard climatology of the study region. These contrasted conditions represent an ideal comparison to investigate some expected effects of climate change. Extensive snow monitoring and pit measurements were performed to contribute to the objectives.

Section 2 presents the study site, the instrumentation, and the observed and estimated physical variables. In Sect. 3, we present the climatology of each winter and the differences in melt rate, snowpack and ground thermal regime, and the evolution of snow cover physical properties within medium-size and small forest gaps and under the canopy. The resulting spring streamflow of the catchment is also presented for both winters in Sect. 3. Finally, we compare our results with existing literature, present the limitations of the study, and discuss the potential climatic, hydrological, and ecological implications of warmer winters in a discontinuous humid boreal forest in Sect. 4.

2 Methods

2.1 Study site

The study took place in the Montmorency Forest (MF) during winters 2020–2021 (W20–21) and 2021–2022 (W21–22). Measurements began on 15 October and ended on 15 June of the following year. MF is located in the province of Québec, in eastern Canada, at the southern edge of the boreal forest (47.29° N, 71.17° W; Fig. 1a).

https://doi.org/10.5194/hess-2023-191
Preprint. Discussion started: 31 August 2023

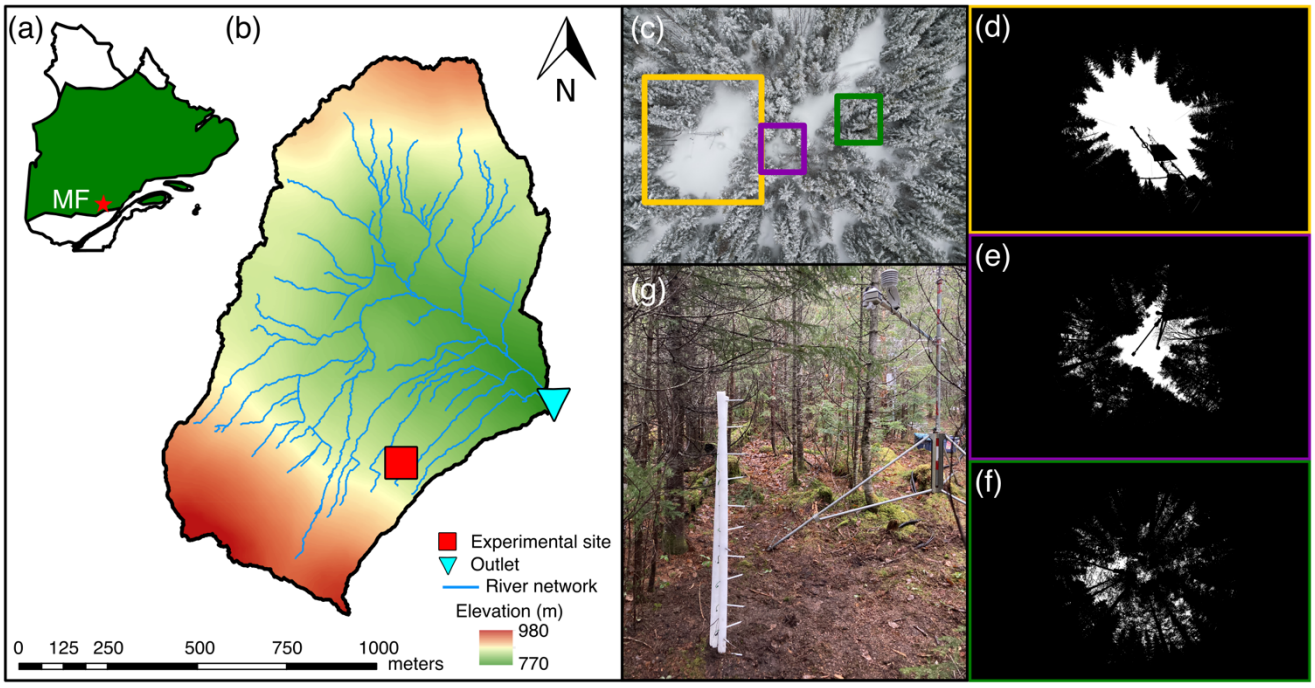

Figure 1: Map of the province of Quebec, Canada, with the location of the Montmorency Forest (MF) indicated by a red star (a). Elevation map of the study catchment (BEREV-7A) with the location of the experimental site and the outlet of the catchment (b). Aerial view of the experimental site with the medium gap (yellow), the small gap (purple), and the canopy (green) stations (c) and black and white hemispherical photos of each station location (d–e–f). Picture of the monitoring station under the canopy (g).

Three monitoring stations were installed in a 1.1 km^2 forested subcatchment (7A) of the *Bassin expérimental du Ruisseau des Eaux-Volées* (BEREV) located at MF (Fig. 1b). The stations were installed in a medium gap, a small gap, and under the canopy (Fig. 1c). Table 1 presents the gap dimensions and the sky-view fraction (SVF) at each site. The SVF was evaluated using an adaptive thresholding algorithm (Jonas et al., 2020) on hemispherical photographs taken with a Sigma 8mm f3.5 EX DG Circular Fisheye lens in the fall of 2022 (Fig. 1d–e–f). Stations were located on a 12°, northeast-facing slope at 846 m above sea level (ASL), within a 10 m tall stand of balsam fir (*Abies balsamea*) mixed with white birch (*Betula papyrifera*) and white spruce (*Picea glauca*) trees. The catchment is a regeneration from a major logging operation that took place in 1993 (Guillemette et al., 2005). The soil is a sandy loam topped by ≈7 cm of litter. The stations were located in the vicinity of a 15 m flux tower measuring shortwave (0.3–2.8 µm) and longwave (4.5–42 µm), upwelling and downwelling radiation (CNR4; Kipp & Zonen). A V-notch streamflow gauge and a bubble flowmeter, maintained by the provincial government and in operation since 1967, are located at the outlet of the catchment (DEH station 051004, https://www.cehq.gouv.qc.ca/hydrometrie/historique_donnees/). Based on LiDAR imagery, we estimate that 75 % of the catchment is canopy-covered, with the remainder being gaps of small and medium size. Four kilometers northeast of BEREV-7A, there is a 0.01 km^2 open area at 664 m ASL, the NEIGE site (Pierre et al., 2019), which hosts a federal weather station (ECCC station 7042395). We used data from the federal station to position the winters of 20–21 and 21–22 in relation to the

https://doi.org/10.5194/hess-2023-191
Preprint. Discussion started: 31 August 2023

Hydrology and Earth System Sciences
Discussions

Stations	Gap dimensions (m × m)	Sky-view fraction (0 –1)
Medium gap	10 × 14	0.26
Small gap	2 × 3	0.10
Canopy	-	0.08

Table 1: Gap dimensions and sky-view fraction of each station

MF climatology. The NEIGE site also hosts a CS725 instrument (Campbell Scientific) that monitors the snow water equivalent (SWE) at a 6 h timestep, using differential gamma-ray absorption (Choquette et al., 7-11 October 2013) and an ultrasonic snow height sensor (Judd Communication) working on an hourly timestep.

2.2 Measurements of physical variables

In this study, the monitoring stations tracked the thermal regime of the snowpack and of the top 20 cm of soil, the soil volumetric water content (VWC) and the effective thermal conductivity of the snow (k_s) at two levels in the snowpack. Measurements from the stations were complemented with snow pit observations of snow density (ρ_s), temperature, SSA, and a visual identification of the snowpack stratigraphy conducted periodically during both winters.

2.2.1 Monitoring Stations

Each station includes a snow height sensor, either the Judd model or the SR50a from Campbell Scientific, mounted 3 m above the ground, and is equipped with a vertical array of PT1000 thermistors (Schneider Electric). Temperature was measured at depths of 20, 10 and 5 cm in the soil, at the ground surface and then every 15 cm in the snowpack until a maximum height of 180 cm. Thermistors were inserted into white-painted aluminum tubes held in place by a vertical UHMW plastic rod. Snow surface temperature was measured at each station with an SI-111 infrared radiometer (Apogee Instruments) mounted at the same level as the snow height sensor. Each station was also equipped with an HMP60 (Campbell Scientific) sensor that measured air temperature and relative humidity at a height of 3 m above the ground. A CS655 reflectometer (Campbell Scientific) measured the VWC at a depth of 15 cm into the soil. Variations in 15 cm VWC were used as a proxy for infiltration. A CR10X data logger (Campbell Scientific) recorded point measurements every hour. Also, time-lapse cameras taking hourly photos were used to visually identify the precipitation phase and the burying of the thermistors. An example of a monitoring station, the one under the canopy in this case, is presented in Fig. 1g.

The stations were also equipped with two heated TP08 needle probes (NP; Hukseflux) to measure k_s following Morin et al. (2010) and Domine et al. (2015). The lowest NP was installed 10 cm above the ground at each station, whereas the highest NP was installed 65 cm above the ground under the canopy, and 80 cm in the forest gaps to account for the greater snow height in these environments. To prevent snow melting around the heated needle during measurements, these were taken only every other day between 5:00 and 6:00 AM, only when the snow temperature was below –2.5°C. During each measurement, the NP was heated for 150 s with a power of 0.45 W m^{-1}. The heating curve was recorded on a CR1000 data logger (Campbell Scientific). The algorithm developed to automatically assess k_s from the heating curves is derived from Domine et al. (2015)

https://doi.org/10.5194/hess-2023-191
Preprint. Discussion started: 31 August 2023


Hydrology and Earth System Sciences
Discussions

and is described in the Supplementary Material (Fig. S1). The error associated with snow thermal conductivity measurements with these static needle probes is estimated to be 21 % (Domine et al., 2015).

2.2.2 Data gap filling

Small data gaps (1 to 5 h) in the snow height and temperature time series were filled by linear interpolation. We used data from the other stations to fill the longer data gaps, as described in the Supplementary Material (Fig. S2 – S4). This approach was applied to snow height in the medium forest gap (37 days in 2020) and under the canopy (77 days in 2022), to snow surface temperature in the small forest gap (winter 2021–22), and to air and snow surface temperatures under the canopy (16 days in 2022).

2.2.3 Snow pit measurements

Four snow pits were dug in medium gaps, small gaps and under the canopy each winter, for a total of 24 snow pits over the two winters. Snow pits in gaps and under the canopy were all dug at sites with similar conditions (gap size, SVF) to the monitoring stations, all within 150 m of the stations. Table 2 lists the date of each snow pit measurement.

For each snow pit survey, we measured ρ_s with a Snow-Hydro 100 cm^3 box with a ±10% accuracy (Conger and McClung, 2009). Snow density was measured every 3 to 5 cm in the vertical direction. In the presence of ice columns, measurements were taken adjacently. We measured snow temperature using a Greinsinger PT-1000 probe (resolution: 0.1 °C) every 5 cm in the topmost 40 cm of snow and every 10 cm for the lower snow layers. The SSA, being a quantitative indicator of snow metamorphism (Taillandier et al., 2007), was measured using the DUFISSS instrument (Gallet et al., 2009). DUFISSS uses infrared reflectance of snow samples with an integrating sphere at 1310 nm to estimate the SSA with an accuracy of approximately 12% (Gallet et al., 2009). Measurements were taken vertically every 1 to 5 cm depending on the stratigraphy.

	Medium gap	Small gap	Canopy
Winter 2020–21 (low-snow)	8 Dec. 20	8 Dec. 20	8 Dec. 20
	27 Jan. 21	27 Jan. 21	26 Jan. 21
	9 Mar. 21	10 Mar. 21	10 Mar. 21
	6 Apr. 21	6 Apr. 21	6 Apr. 21
Winter 2021–22 (reference)	13 Jan. 22	12 Jan. 22	12 Jan. 22
	15 Feb. 22	15 Feb. 22	15 Feb. 22
	10 Mar. 22	11 Mar. 22	10 Mar. 22
	28 Apr. 22	29 Apr. 22	28 Apr. 22

Table 2: Snow pit measurement dates

https://doi.org/10.5194/hess-2023-191
Preprint. Discussion started: 31 August 2023


Hydrology and Earth System Sciences
Discussions

2.3 Estimated variables

2.3.1 Snow water equivalent and snowpack cold content

We estimated the SWE (m) from snow density profiles using:

$$SWE = \frac{h\overline{\rho_s}}{\rho_w}, \quad (1)$$

where h and $\overline{\rho_s}$ are respectively the height (m) and the average density (kg m^{-3}) of the snowpack, and ρ_w is the density of liquid water (1000 kg m^{-3}).

The snowpack cold content (Q_{CC}, in J m^{-2}) is the quantity of energy needed to bring the snowpack to its melting point. It is defined as:

$$Q_{CC} = -c_{ice} \sum_{i=1}^{n} h_i \, \overline{\rho_{s,i}} \, (\overline{T_{s,i}} - T_m), \quad (2)$$

where c_{ice} is the heat capacity of ice (2108 J kg^{-1} K^{-1}), h_i and $\overline{\rho_{s,i}}$ are the same as above but for a given snow layer i. $\overline{T_{s,i}}$ is the average temperature between the bottom and top boundaries of each i layer (K) as monitored at the stations and T_m is the melting point of ice (273.15 K). h_i corresponds to the vertical distance between each temperature measurements.

Since snow density profiles were point measurements, we interpolated $\overline{\rho_{s,i}}$ linearly between each snow pit date at an hourly timestep to match temperature monitoring. Snow density was assumed constant from the beginning of the snow season until the date of the first snow pit (23 days in W20–21 and 59 days in W21–22) and then from the last snow pit date until the melt-out (39 days in W20–21 and 31 days in W21–22). To validate this rough hypothesis, we measured four density profiles in W20–21 and five in W21–22 at NEIGE site next to the SWE sensor and compared the resulting estimated SWE time series with direct observations, as shown in the Supplementary Material (Fig. S5).

2.3.2 Snowpack net shortwave and longwave radiation

We used the HPEval model (Jonas et al., 2020) to estimate the downwelling shortwave radiation below the canopy ($SWR_{\downarrow,bc}$) from the hemispherical photographs taken at the monitoring stations and the incoming shortwave radiation measured above the canopy at the flux tower, some 10 m away. HPEval combines hemispherical imagery of the canopy and radiation transfer modeling to estimate subcanopy shortwave radiation at very high spatial and temporal resolution. Reflected shortwave radiation by the snowpack ($SWR_{\uparrow,bc}$) was estimated using five arbitrary albedo classes defined from the work from Hardy et al. (2000) and Melloh et al. (2001). The five classes are listed in Table 3.

We manually assigned a daily albedo class to the snow surface by visually inspecting timelapse photographs from each station. A sample representative photo of each albedo class is presented in Figure S6. The net shortwave radiation below canopy ($SWR_{net,bc}$) is the difference between $SWR_{\downarrow,bc}$ and $SWR_{\uparrow,bc}$.

https://doi.org/10.5194/hess-2023-191
Preprint. Discussion started: 31 August 2023

Hydrology and Earth System Sciences
Discussions

Class	Albedo	Description
1	0.80	Dry snow
2	0.70	Dry snow with litter and/or rough surface
3	0.65	Wet snow
4	0.55	Wet snow + litter
5	0.40	Wet snow + lots of litter

Table 3: Albedo classes used for the estimation the reflected shortwave radiation by the snow surface

We estimated the downwelling longwave radiation below the canopy ($LWR_{\downarrow,bc}$; W m^{-2}) by using:

$$LWR_{\downarrow,bc} = SVF \times LWR_{\downarrow,ac} + (1 - SVF)\, \varepsilon_{can}\, \sigma\, {T_{can}}^4 , \quad (3)$$

where $LWR_{\downarrow,ac}$ is the downwelling longwave radiation measured above the canopy at the nearby flux tower (W m^{-2}), σ is the Stefan–Boltzmann constant (5.67 × 10^{-8} W m^{-2} K^{-4}), ε_{can} is the canopy emissivity, set to 0.98 (Pomeroy et al., 2009), and T_{can} is the canopy temperature (K). We assume that the canopy temperature can be approximated by the air temperature measured at our monitoring stations.

The upwelling longwave radiation below the canopy ($LWR_{\uparrow,bc}$; W m^{-2}) is determined with:

$$LWR_{\uparrow,bc} = \varepsilon_s\, \sigma\, {T_{surf}}^4 , \quad (4)$$

where ε_s is the emissivity of the snow surface, set to 0.99 (Sicart et al., 2006), and T_{surf} is the snow surface temperature (K) measured at each station. The net longwave radiation below canopy ($LWR_{net,bc}$) is the difference between $LWR_{\downarrow,bc}$ and $LWR_{\uparrow,bc}$. The net total radiation below canopy ($R_{net,bc}$) is the sum of $SWR_{net,bc}$ and $LWR_{net,bc}$.

2.3.3 Ground heat flux

The ground heat flux was assumed equivalent to the snow heat flux within the lower 15 cm of the snowpack (Lackner et al., 2022), and calculated using Fourier's law (Eq. 5).

$$F = -k_s \frac{(T_{15} - T_0)}{dh} , \quad (5)$$

where F (W m^{-2}) is the heat flux of the lower 15 cm of the snowpack, k_s (W m^{-1} K^{-1}) is the effective thermal conductivity of this basal snow layer, taken as the NP measurement at a 10 cm height, T_{15} and T_0 are the temperatures measured 15 cm above the ground and at the ground surface (K), respectively, dh is the thickness of the bottom layer (15 cm). To avoid melting of the ice matrix, NPs were not heated when the snow was warmer than –2.5°C. Because of this constraint, k_s at 10 cm from each station was only measured at the beginning of the winter on both years when the bottom of the snowpack was colder than –2.5°C. This resulted in more than 80% k_s measurements that were missing. In order to have complete time series of k_s, we used Eq. 18 from Fourteau et al. (2021) with our pit density measurements to estimate k_s. We validated the use of this empirical equation by comparing it to our observations of pit density and monitoring of k_s at 10 and 65 or 80 cm at all stations. We used

https://doi.org/10.5194/hess-2023-191
Preprint. Discussion started: 31 August 2023


Hydrology and Earth System Sciences
Discussions

k_s that was measured the closest in time to the snow pit surveys. Before comparing our observations with the equation, correction factors between 1.1 and 1.3, depending on snow temperature, were applied to k_s measurements to account for the systematic underestimation of the fixed NP approach (Fourteau et al., 2022). Doing this, we found a correlation coefficient of 0.70 and a bias of 10.2% between our observations and the equation from Fourteau et al. (2021). Comparison between the corrected measurements and the equation is detailed in the Supplementary Material (Fig. S7).

2.3.4 Vertical temperature gradient

The magnitude of the mean snowpack vertical temperature gradient ($|\partial T/\partial z|$; in °C m^{-1}) is expressed as follow:

$$|\partial T/\partial z| = \left|\frac{(T_{surf}-T_0)}{h_s}\right|, \quad (6)$$

where ($T_{surf} - T_0$) is the temperature difference between the snow surface and the soil–snow interface (in °C) and the h_s is the snow height (in m).

2.3.5 Snow permeability

Snow permeability (K_s; in m^2) indicates the ease with which a fluid subjected to a pressure gradient flows through a porous medium. K_s can be estimated from ρ_s and the optical grain radius (r_g; in m) according to the following equation (Calonne et al., 2012):

$$K_s = 3{r_g}^2 e^{-0.013\rho_s}. \quad (7)$$

We assume that each snow layer is a collection of independent ice spheres (ρ_{ice} = 917 kg m^{-3}) with the same SSA as the snow of interest (Grenfell and Warren, 1999). Therefore, r_g is estimated as follow:

$$r_g = \frac{3}{\rho_{ice} SSA}. \quad (8)$$

3 Results

3.1 Climatic conditions

Figure 2 shows the monthly sum of precipitation and the mean of the monthly air temperature from October to May, as recorded at the NEIGE site in W20–21 and W21–22 compared with the average over 1982–2022. W20–21 was the driest winter of the 1982–2022 period, with 199 mm recorded from January to April (JFMA), including 167 mm of solid precipitation (Table 4). This corresponds to a precipitation anomaly of –224 mm. In comparison, the JFMA anomaly of precipitation in W21–22 was only +5 mm. December–January–February (DJF) temperature in W20–21 was also 2.8°C warmer than the 1982–2022 average. As for DJF, W20–21 was the fourth warmest year of the last 40 years. In comparison, DJF temperature was 1.8°C colder in W21–22 than the 1982–2022 average and ranks as the sixth coldest for that period. The exceptionally dry and warm winter of

https://doi.org/10.5194/hess-2023-191
Preprint. Discussion started: 31 August 2023

Hydrology and Earth System Sciences
Discussions

2020–21 resulted in the earliest melt-out in the last 40 years at NEIGE site (11 April 2021), with snow disappearing 23 days earlier than the 1982–2022 average (Table 4). Two heavy rain-on-snow (ROS) events were observed in December 2020, three smaller ones in November and December 2021, and several others in March, April, and May of both years. As the data show, the winter 2020–21 received a much lower than average solid precipitation and was significantly warmer resulting in a thin snowpack. We will refer to it as our low-snow and warm winter. The precipitation and temperature anomaly in the winter of 2021–22 is much weaker. Therefore, W21–22 will correspond to the reference winter for the rest of the analysis.

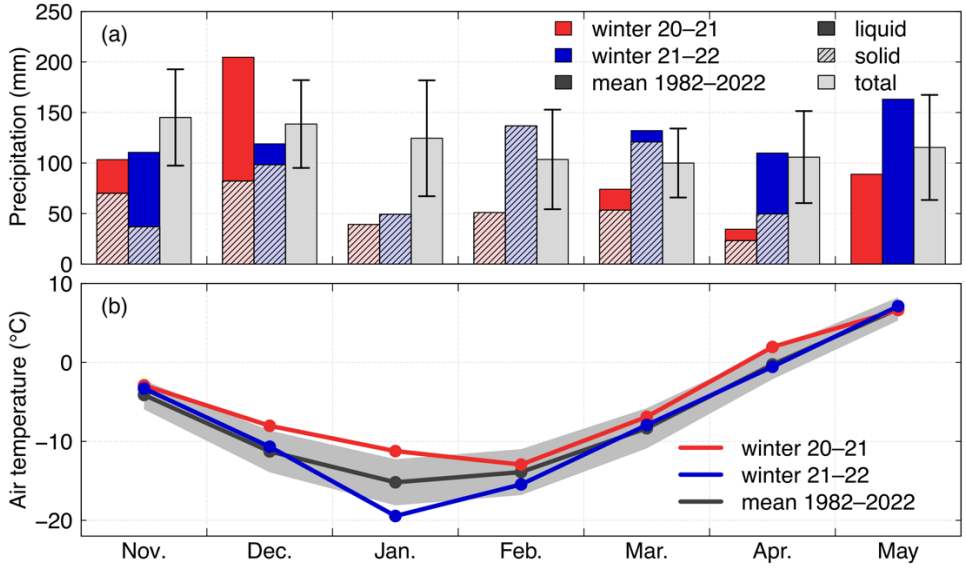

Figure 2: Monthly sum of precipitation (a) and means of air temperature (b) from November to May in the winters of 2020–21 and 2021–22, measured at the NEIGE site and compared to the monthly sum of precipitation and means of hourly temperature over the 1982–2022 period. Dashed bars in (a) show snowfall whereas solid bars indicate rainfall. The standard deviation of the 1982–2022 is shown by the black error bars for precipitation in (a) and by the gray area for the monthly temperature in (b).

	Winter 2020–21			Winter 2021–22		
	value	anomaly	rank (out of 40)*	value	anomaly	rank (out of 40)*
P_{tot} JFMA (mm)	199	–224	1	428	+5	16
P_{tot} (Nov-May)	596	–237	2	821	+12	19
P_{sol} (Nov-May)	364	–198	2	596	+13	19
Temp. DJF (°C)	–10.7	+2.8	4	–15.2	–1.8	31
$H_{s,max}$ (cm)	67	–38	5	142	+37	33
Melt-out day (DOY)	101	–23	1	134	+11	33

* Temp. DJF is ranked in descending order, whereas all the other variables are ranked in ascending order.

Table 4: Total precipitation from January to April (JFMA) and from November to May, solid precipitation from November to May, mean December-January-February (DJF) temperature, maximum recorded snow height ($H_{s,max}$), and the melt-out day at the NEIGE site for the 2020–21 and 2021–22 winters. The anomaly relative to the 1982–2022 period is also shown, along with the rank of both winters for each metric relative to the 40 winters of the climatology. We used a threshold at 1°C to define the precipitation phase over the analysis period. Winters 1999 to 2003 were excluded of the analysis because of too many missing data.

https://doi.org/10.5194/hess-2023-191
Preprint. Discussion started: 31 August 2023


Hydrology and Earth System Sciences
Discussions

3.2 Snow accumulation and melt dynamics

Figure 3 shows the evolution of the snowpack thermal regime in gaps and under the canopy, along with the snowpack cold content (Q_{CC}). Due to a lower snowfall, the snowpack in W20–21 was on average 46% thinner than in the reference winter. Since the air was warmer in W20–21, the temperature of the upper snow layers was also higher. In contrast, because there was less snow on the ground in W20–21, heat transfer through the snow was facilitated, resulting in the base of the snowpack being colder in W21–22. Due to canopy interception, less snow accumulated under the trees than in the gaps in both years. Interestingly, topmost snow layers seem to be colder under the canopy than inside gaps. This is in contradiction with Figure 4 that shows snow surface temperature being higher under the canopy than inside gaps at night, despite similar air temperature at all three stations. This discrepancy is further discussed in Sect. 4.2.

https://doi.org/10.5194/hess-2023-191
Preprint. Discussion started: 31 August 2023

Hydrology and Earth System Sciences
Discussions

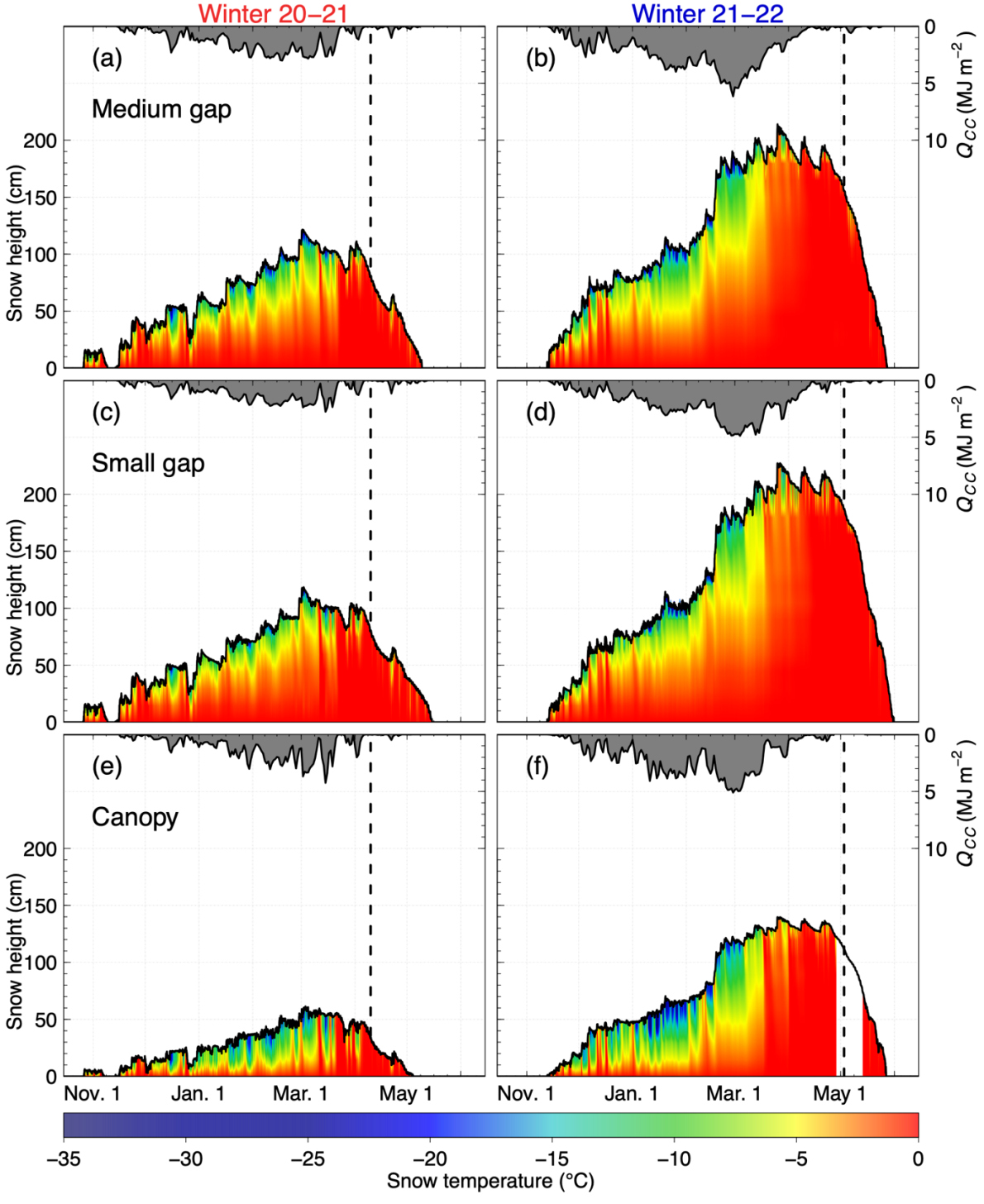

Figure 3: Snowpack thermal regime and cold content in the medium gap (a–b), in the small gap (c–d) and under the canopy (e–f) for winters 2020–21 (left) and 2021–22 (right). Dashed lines show the onset of snowmelt.

https://doi.org/10.5194/hess-2023-191
Preprint. Discussion started: 31 August 2023

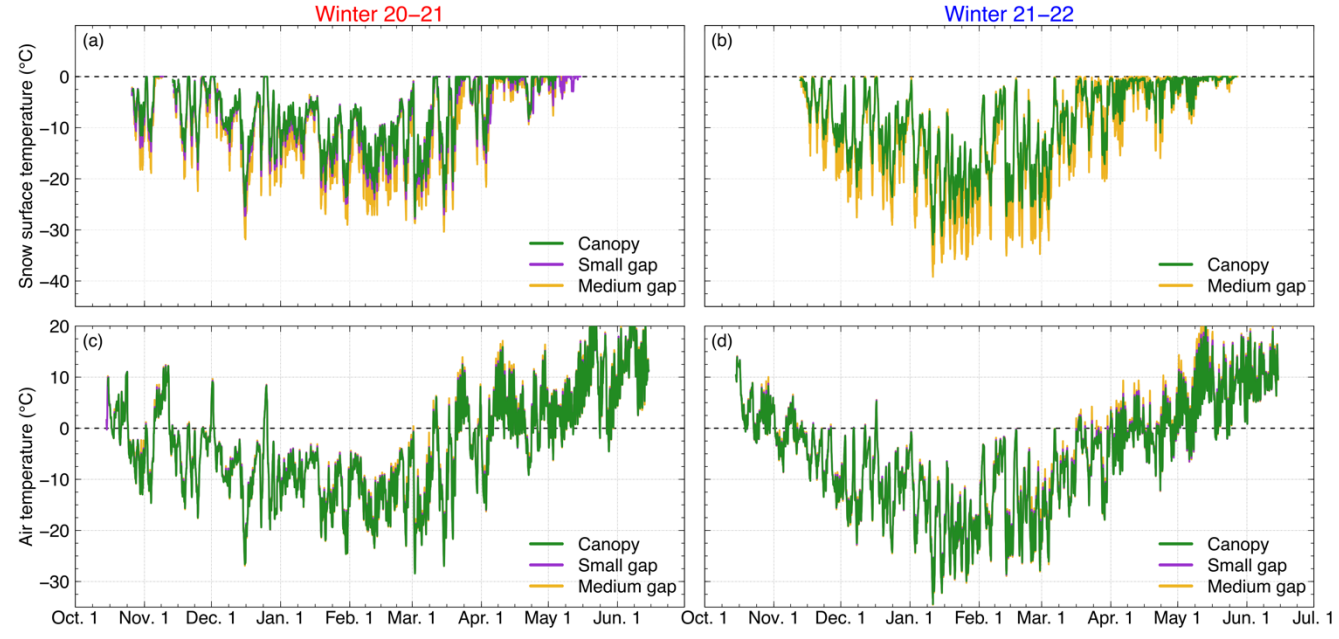

Figure 4: Snow surface and air temperature measured in the medium gap (yellow), in the small gap (purple) and under the canopy (green) during winters 2020–21 (a–c) and 2021–22 (b–d). Since the snow surface temperature in the small gap was entirely gap-filled in winter 21–22, it is not presented in (b).

Due to the thinner snowpack and warmer air temperature, the Q_{CC} was on average 36% lower in W20–21 than in W21–22. Interestingly, the Q_{CC} peaked in late February in both winters. However, since less energy was required to warm the snowpack to 0°C, snowmelt started on average 23 days earlier in the low-snow and warm winter than in the reference winter (10 Avril 2021 vs 3 May 2022), which is a substantial difference. Since the snowpack was thicker in the gaps than under the canopy, the Q_{CC} was slightly less under the trees than in both gaps.

As snowmelt started more than three weeks earlier in W20–21 than in the reference winter, less radiative energy was available to contribute to snowmelt (Fig. 5). Net shortwave ($SWR_{net,bc}$) and longwave ($LWR_{net,bc}$) radiation below canopy were both lower in the low-snow and warm year. As expected, we observed a decrease in $SWR_{net,bc}$ and an increase in $LWR_{net,bc}$ as the sky-view-fraction decreased regardless of the year.

https://doi.org/10.5194/hess-2023-191
Preprint. Discussion started: 31 August 2023

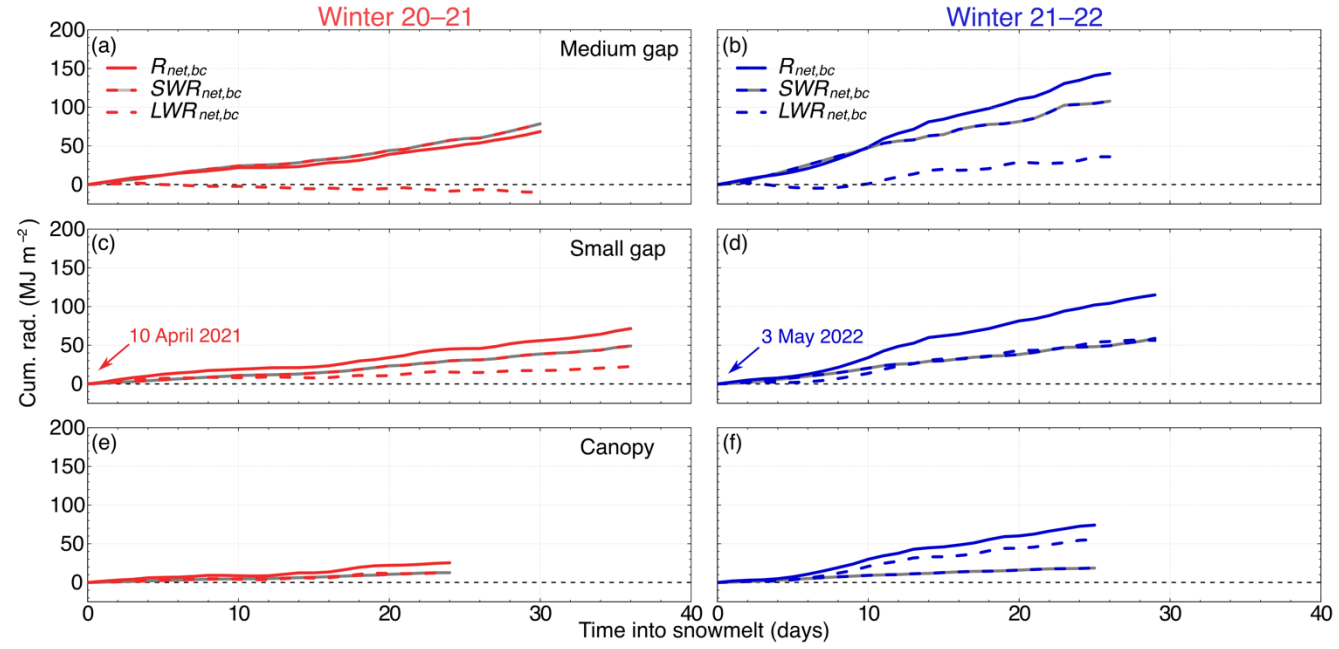

Figure 5: Cumulative net total ($R_{net,bc}$), shortwave ($SWR_{net,bc}$) and longwave ($LWR_{net,bc}$) radiation below the canopy during snowmelt of winter 2020–21 (left) and 2021–22 (right) in the medium gap (a–b), in the small gap (c–d) and under the canopy (e–f). Graphs start at the beginning of the snowmelt period on each year, which differs on average by 23 days between seasons.

Figure 6 shows the evolution of SWE from the beginning of snowmelt in both years. In the medium gap, small gap and under the canopy, the SWE at the beginning of snowmelt in the low-snow year was 56%, 59% and 76% lower, respectively, than in the reference year. In addition to a thinner snowpack, the melt rate was also significantly smaller during the low-snow winter. Overall, from W20–21 to W21–22, the duration of the melt period slightly increased from 26 to 31 days and from 29 to 37 days in the medium and small gaps, respectively, whereas it did not change under the canopy.

https://doi.org/10.5194/hess-2023-191
Preprint. Discussion started: 31 August 2023

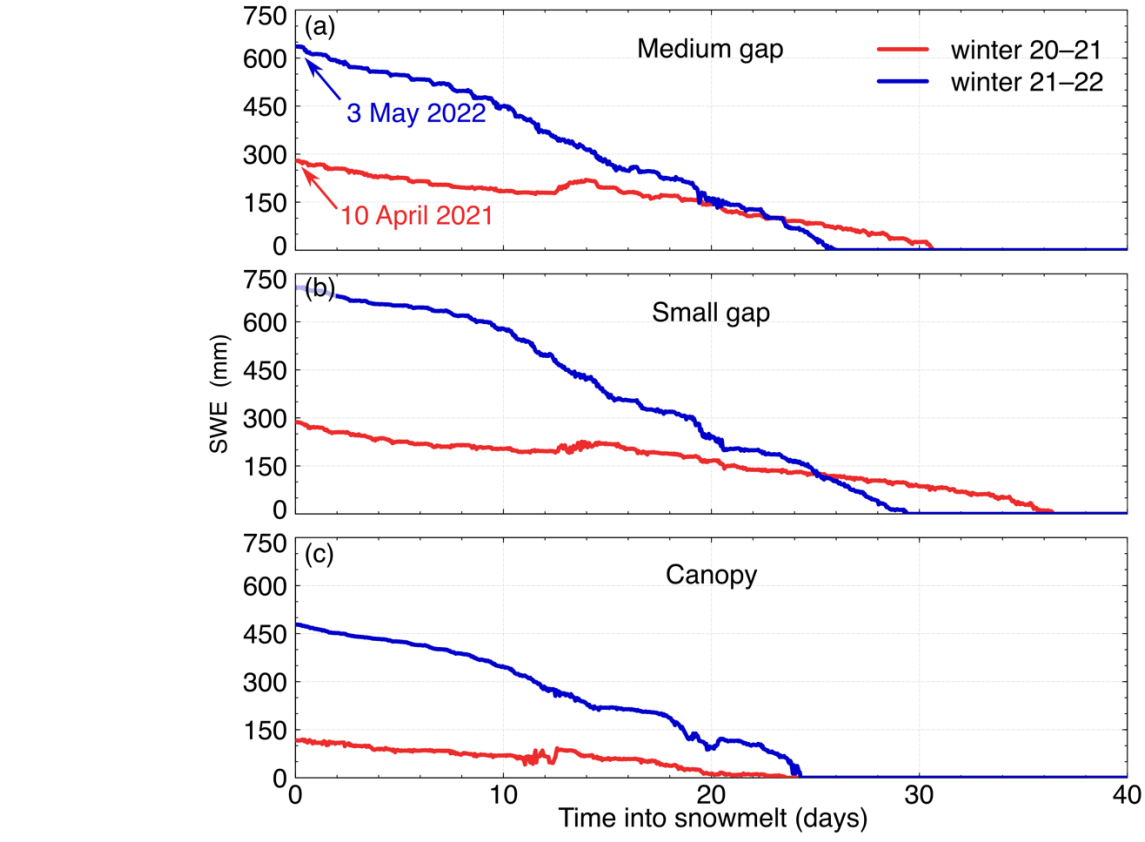

Figure 6: SWE evolution during snowmelt of winters 2020–21 (red) and 2021–22 (blue) in the medium gap (a), in the small gap (b) and under the canopy (c). The plots start at the beginning of the snowmelt period on each year, which differs by an average of 23 days between seasons.

3.3 Ground thermal regime and water content

Figure 7 shows the ground heat flux (GHF) and the soil temperature at several depths in both years. Overall, the GHF in DJF was on average 50% higher in W20–21 than in the reference winter. The largest difference was observed under the canopy, where the GHF was larger than in gaps in W20–21 and in W21–22.

At any given depth, the soil was cooler in W20–21 than in W21–22 in DJF (Fig. 7; Table 5), even though it was a warmer season. In both winters, the top few centimeters of soil below the canopy dropped below freezing, while all soil layers in the gaps remained above or at 0°C. We also observed a frozen soil–snow interface during snow pit surveys under the canopy, but never in the gaps. In the low-snow and warm winter, the freezing depth reached 10 cm, compared to only 5 cm in the reference winter, even though it was much colder. However, the soil–snow interface was below 0°C for similar durations (103 days vs 102 days).

https://doi.org/10.5194/hess-2023-191
Preprint. Discussion started: 31 August 2023

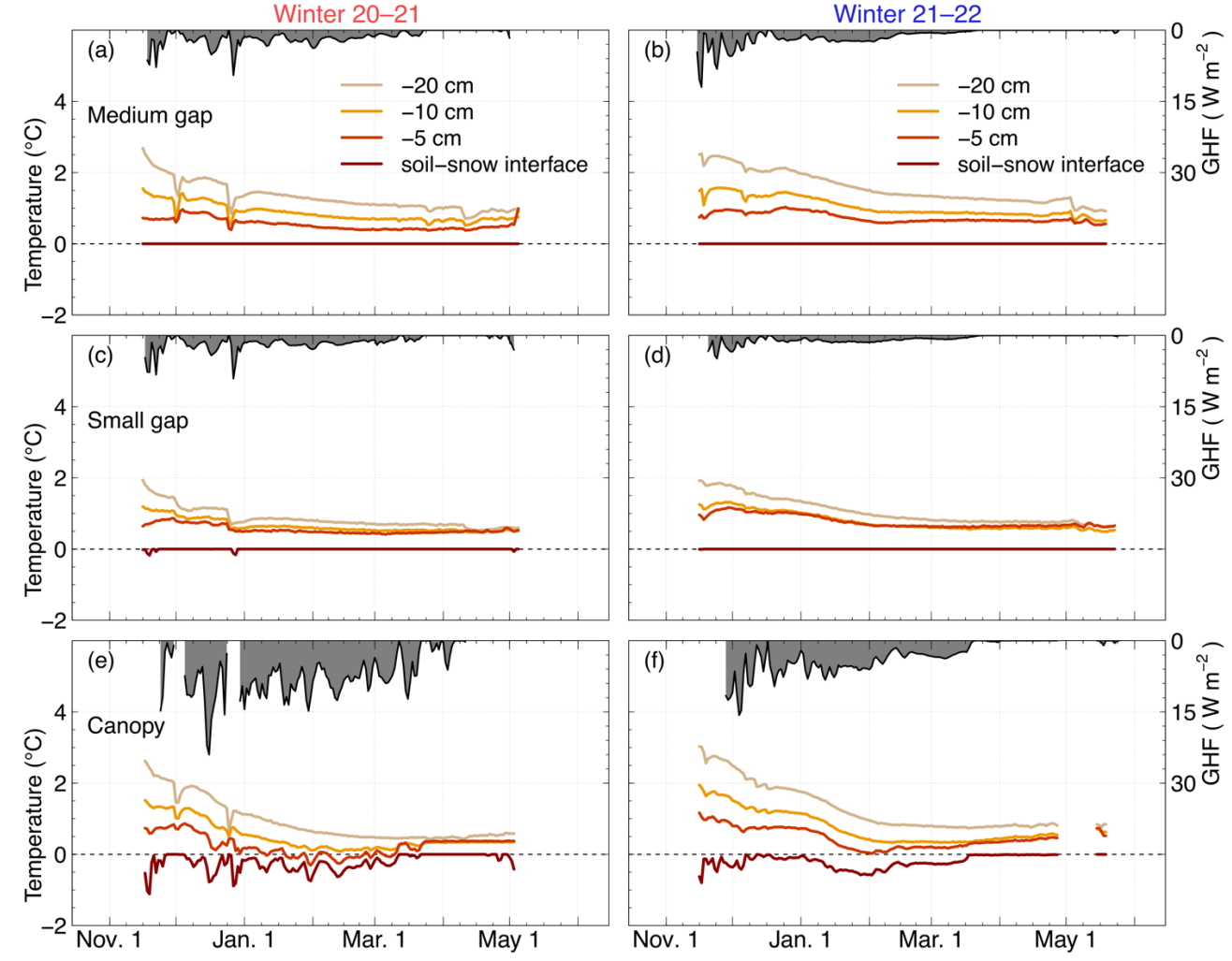

Figure 7: Ground heat flux (GHF) and temperature at 20, 10, 5 cm below ground level and at the soil–snow interface during the snow cover period of winters 2020–21 (left) and 2021–22 (right) in the medium gap (a–b), in the small gap (c–d) and under the canopy (e–f).

	Stations					
	Medium gap		Small gap		Canopy	
Soil Depth	Temp. 20–21 (°C)	Δ*T* (°C)	Temp. 20–21 (°C)	Δ*T* (°C)	Temp.20–21 (°C)	Δ*T* (°C)
Soil–snow interface	0	0	0	0	–0.32	–0.05
5 cm	0.59	–0.20	0.55	–0.29	0.15	–0.28
10 cm	0.92	–0.23	0.67	–0.21	0.49	–0.32
20 cm	1.40	–0.35	0.88	–0.31	1.00	–0.42

Table 5: Mean December–January–February temperature at the soil–snow interface and at 5, 10 and 20 below ground level and at the soil-snow interface in the medium gap, in the small gap and under the canopy for winter 20–21 and the difference with winter 21–22.

https://doi.org/10.5194/hess-2023-191
Preprint. Discussion started: 31 August 2023

Hydrology and Earth System Sciences
Discussions
Open Access
EGU

Figure 8 shows that soil volumetric liquid water content (VWC) at 15 cm depth was higher under the canopy than in gaps for both years, except in spring and after two heavy ROS that occurred early in W20–21. Soil profile characterization that was performed in a small gap and under the canopy during the summer of 2020 showed different porosity in the topmost 30 cm of soil which could explain the differences in VWC over a short distance at our study site. On 10 April 2021 (Fig. 8a), the increase in VWC was sharp and sudden in both gaps, while it was more gradual under the canopy. A data acquisition error occurred at the canopy station in April and May 2022 (Fig. 8b), so we cannot compare the increase in 15 cm VWC under the canopy at the onset of snowmelt in W20–21 and W21–22. In the medium and small gaps, we observed a similar behavior of the 15 cm VWC at the beginning of snowmelt in 2022.

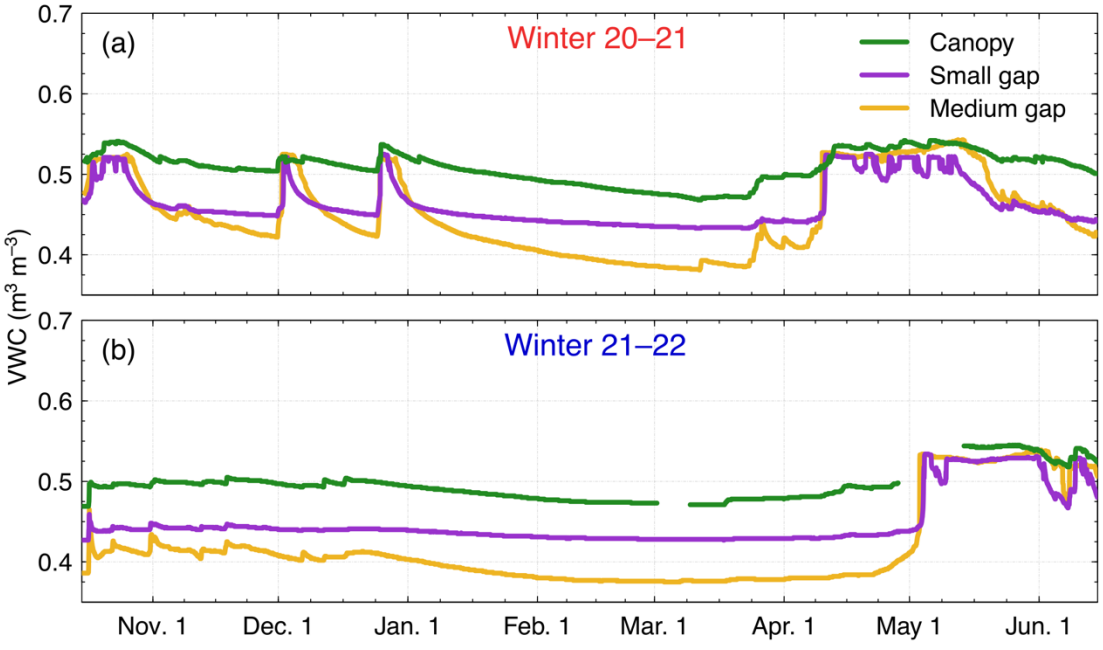

Figure 8: Soil liquid water content (VWC) at 15 cm below the surface in the medium gap (yellow), in the small gap (purple) and under the canopy (green) in winters 2020–21 (a) and 2021–22 (b).

3.4 Vertical temperature gradient and snow properties

Figure 9 shows the magnitude of the vertical snow temperature gradient ($|\partial T/\partial z|$) between the snow surface and the ground. $|\partial T/\partial z|$ decreased throughout the season in both winters. From November to January, the average $|\partial T/\partial z|$ was similar at each site and year. In February and March of the low-snow and warm winter, $|\partial T/\partial z|$ remained within or above the transition zone from equilibrium to kinetic crystal growth (Colbeck, 1983). In contrast, in February of the reference winter, the decrease of $|\partial T/\partial z|$ was more intense and we observed a drop of $|\partial T/\partial z|$ below 10°C m^{-1} in gaps. $|\partial T/\partial z|$ was also higher under the canopy than in gaps.

https://doi.org/10.5194/hess-2023-191
Preprint. Discussion started: 31 August 2023

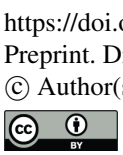

Hydrology and Earth System Sciences
Discussions
Open Access
EGU

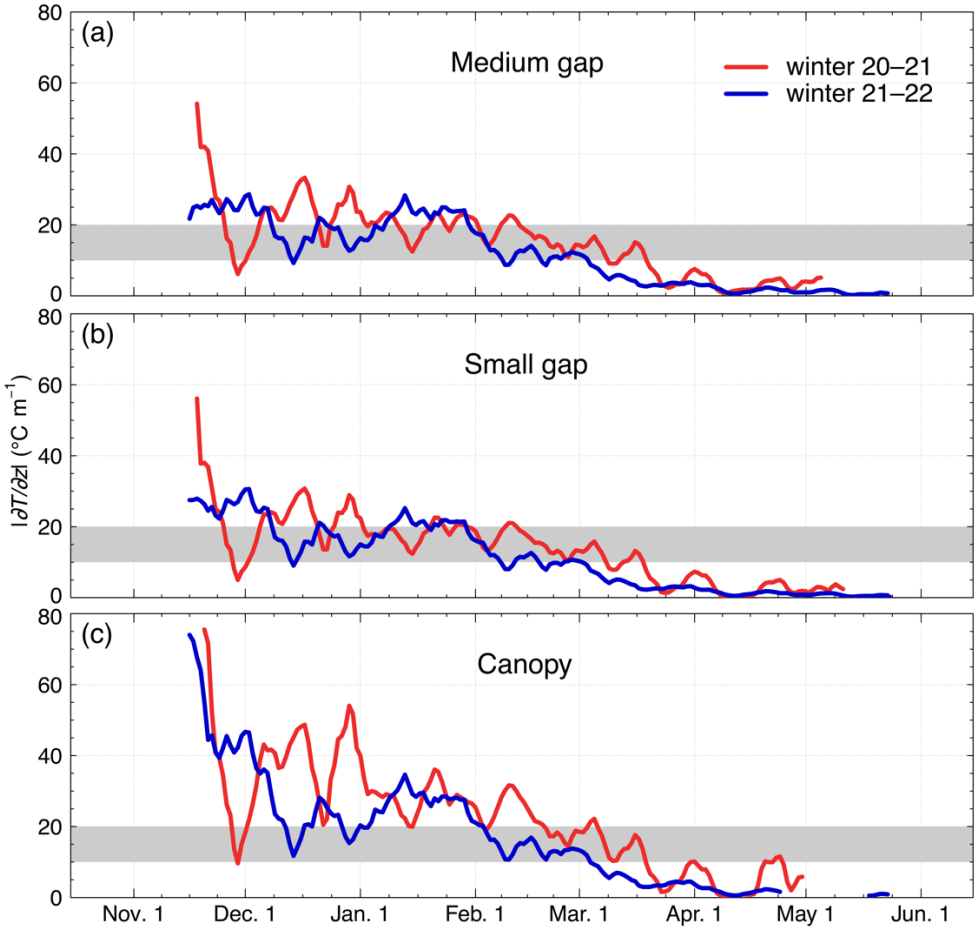

Figure 9: 7 day rolling mean of the magnitude of the vertical temperature gradient ($|\partial T/\partial z|$) in winters 2020–21 (red) and 2021–22 (blue) in the medium gap (a), the small gap (b) and under the canopy (c). The grey band on each frame shows the transition zone from equilibrium to kinetic growth.

Figure 10 presents the comparison of snow stratigraphy, density, SSA and permeability between both years for gaps and under the canopy as obtained from snow pit observations between 9 and 11 March both years. These snow pit dates are convenient to present as they are similar in both years and correspond to a snowpack under dry snow conditions and well into the snow accumulation period. Observations from the other snow pits are presented in Supplementary Material (Fig S8 – S11).

At all sites, there was a greater proportion of faceted crystals (FC) and depth hoar (DH) in the snowpack during the low-snow year than during the reference year. In contrast, we observed fewer rounded grains (RG) in W20–21 than in W21–22. In both years, FC and DH layers were proportionally thicker under the canopy than in the gaps. A thick layer of melt-freeze polycrystals (MFpc) was observed at the base of the snowpack in W20–21 as a result of the December 2020 ROS. Also, in W20–21, we observed ice layers (IL) and melt-freeze crusts (MFcr) in the gaps, but not under the canopy. In W21–22, a thin MFpc was observed at the base of the snowpack. Three to four IL and MFcr were also observed within the gap and canopy snowpacks.

https://doi.org/10.5194/hess-2023-191
Preprint. Discussion started: 31 August 2023

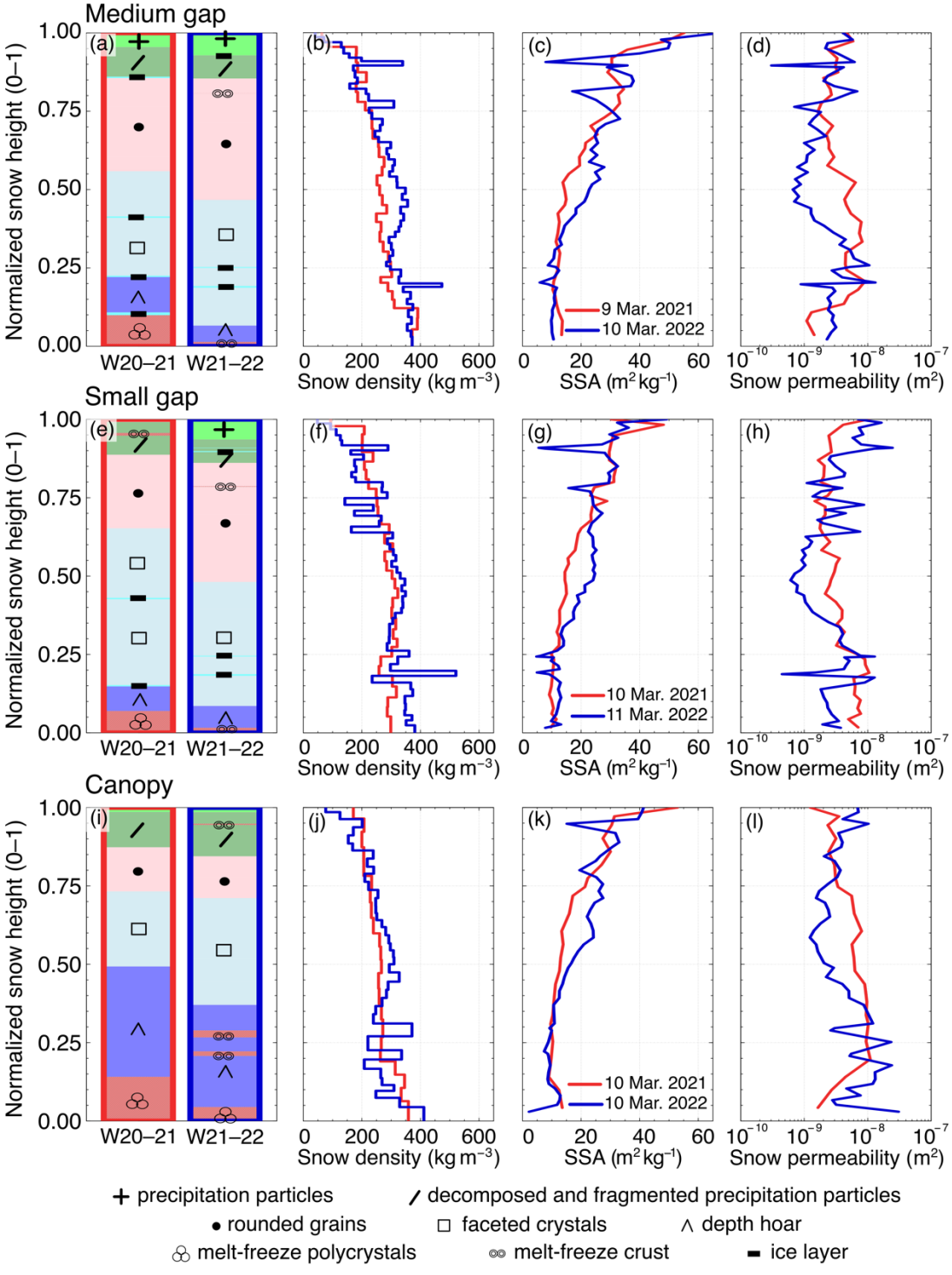

Figure 10: Stratigraphy, snow density, SSA, and snow permeability profiles as measured in the medium gap (a–b–c–d), in the small gap (e–f–g–h) and under the canopy (i–j–k–l) on 9 and 10 March 2021 (red) and 10 and 11 March 2022 (blue).

https://doi.org/10.5194/hess-2023-191
Preprint. Discussion started: 31 August 2023


Hydrology and Earth System Sciences
Discussions

Snow density was lower in W20–21 than in the reference winter (257 kg m^{-3} versus 276 kg m^{-3} on average). In general, the density profiles showed values increasing with depth and were lower under the canopy than in gaps in both winters. A Kruskal–Wallis test performed on density measurements from all sites showed that the density difference between both winters was significant (p-value < 0.05).

The vertical profile of SSA followed the expected general shape, with higher values near the surface (fresh snow) and lower values deeper (FC and DH). In the bottom 25% of the snowpack, there was no significant difference in SSA between both winters (p-value < 0.05). This may be due to the ice and melt-freeze layers SSA measurement technique that was improved from W20–21 to W21–22. Removing the ice and melt-freeze layers from the analysis leads to a significantly greater SSA in W21–22, coherent with a lower temperature gradient. At a normalized height of 0.25 to 0.75, where the transition from RG to FC occurred, the SSA was 19% lower during the low-snow winter than in the reference winter, which was statistically significant (p-value < 0.05). As a result of a lower density and SSA, the snow permeability was 57% higher in the warm and low-snow winter within the height range 0.25 to 0.75. This difference between both years was also statistically significant, as demonstrated by a Kruskal–Wallis test (p-value < 0.05). Note that in both years, the SSA and the snow permeability was lower and higher, respectively, under the canopy than in gaps.

3.5 Spring streamflow

Figure 11 shows the evolution of air temperature and precipitation from the NEIGE site, the decrease in SWE estimated at the monitoring stations and the hydrographs from measurements of spring streamflow at the outlet of the BEREV-7A catchment in April and May of both years. In 2021, air temperatures became positive in early April, allowing a decline in SWE. In 2022, this occurred 20 days later. The daily melt rate was much smaller in the first winter than in the second, as already shown in Fig. 6. The April and May precipitation was also lower in 2021 compared to the following year (122 mm vs 253 mm).

As shown in Fig. 11e–f, spring discharge began to increase on April 7 during the low-snow and warm winter, and began to rise on 1 May, 24 days later, during the reference winter. The spring freshet was earlier than the median spring hydrograph in W20–21, and slightly later in W21–22. The peak discharge in the low-snow winter was similar to the peak of the median hydrograph but was a factor of 5 lower than in W21–22. In both winters, the peak discharge was measured during a day with snowmelt and heavy precipitation (Fig. 11c–d). Low snowmelt and precipitation water inputs in the first winter resulted in significantly lower spring runoff volumes than in the reference winter. In April and May 2021, 2.1×10^5 m^3 flowed out of the catchment compared to 5.7×10^5 m^3 in the following year. The spring runoff volume from the low-snow and warm winter was the lowest volume observed at the outlet of BEREV-7A for April and May since discharge monitoring began in 1968. In 2022, it was the sixth highest.

https://doi.org/10.5194/hess-2023-191
Preprint. Discussion started: 31 August 2023

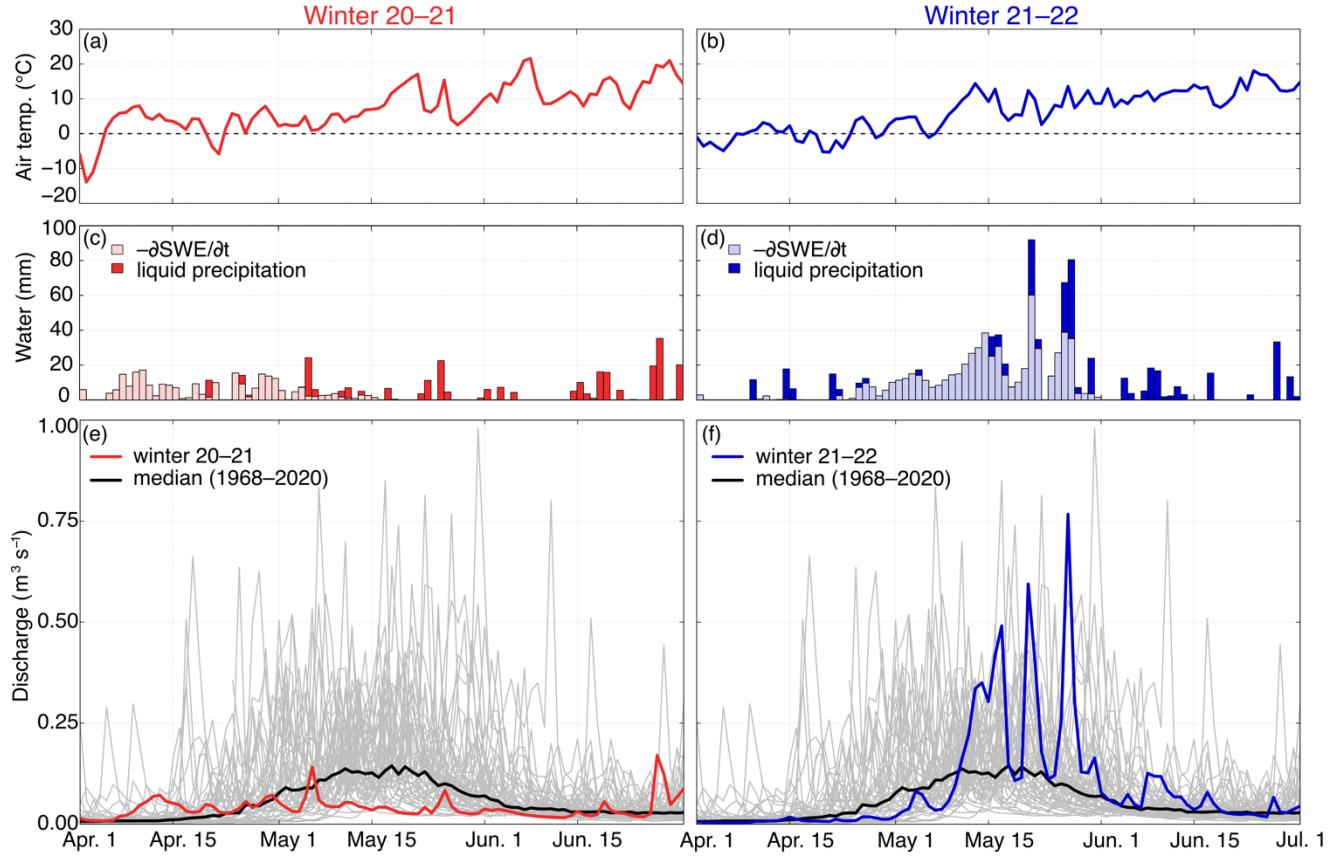

375 **Figure 11: Air temperature (a–b), daily difference of SWE, total precipitation (c–d) and streamflow discharge (e–f) for winter 20-21 (left) and 21-22 (right). Air temperature and precipitation are measured at the NEIGE site, some 4 km north of the main study site, SWE is averaged for the canopy (75%), small gap (12.5%) and medium gap (12.5%) stations for representativeness of the study catchment, and the discharge is monitored at the outlet of the BEREV-7A catchment. The grey lines and the black curve and in (e) and (f) show historical measurements and the median discharge, respectively, over the 1968–2022 period.**

380 **4 Discussion**

So far, our observations show that the low-snow and warm winter of 2020–2021 led to a slower melt, colder ground, enhanced gradient metamorphism and ultimately to a reduced and less intense spring freshet than the reference winter of 2021–2022. However, there are important nuances to consider with respect to forest gaps and subcanopy snowpacks. Figure 12 provides a conceptual summary of our observations.

https://doi.org/10.5194/hess-2023-191
Preprint. Discussion started: 31 August 2023

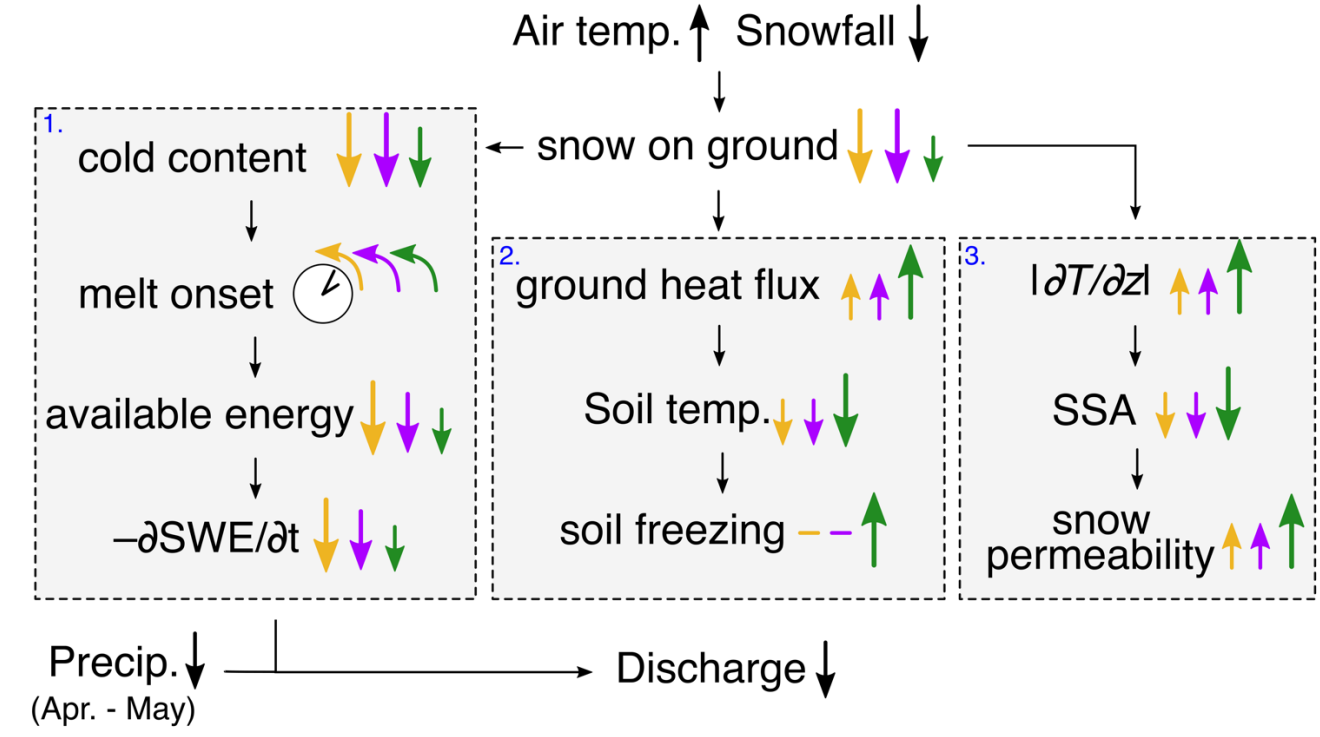

Figure 12: Summary of the results. Upward arrows correspond to an increase and downward arrows to a decrease in the low-snow and warm winter with respect to the reference winter. The clock with counterclockwise arrows means that the process happens earlier. The yellow, purple, and green arrows indicate the effects in the medium gap, the small gap and under the canopy, respectively. Their relative size shows the importance of the process between the gaps and the subcanopy locations. Large black arrows are applied all three locations. Small black arrows show the causal link between the observations processes. Gray boxes refer to processes treated in this study (1. snowmelt dynamics; 2. soil thermal regime; 3. snow metamorphism).

4.1 Low-snow and warm winter

In eastern Canada, as in high-latitude and high-altitude regions, less solid precipitation and higher temperatures are expected in winter with climate change, leading to a reduction in snow cover extent (Guay et al., 2015; Ouranos and MELCCFP, 2022; Pepin et al., 2015; Kunkel et al., 2016). Winter 2020–21 at MF received 211 mm less solid precipitation and was warmer by 4.6°C in DJF, and snow melt-out occurred 34 days earlier than in 2021–22, which is more representative of the prevailing local climatic conditions (Fig. 2; Table 4). Indeed, W20–21 was exceptional in that it had both the lowest snowfall in the last 40 years and was one of the warmest winters in that period (ranked fourth). In contrast, W21–22 was a relatively cold winter with an anomaly of –1.8°C compared to the 1982–2022 period, with solid precipitation close to the climate normals. Another feature of global warming in eastern Canada is an increase in the occurrence and intensity of ROS events (Vincent and Mekis, 2006; Il Jeong and Sushama, 2018). Although there were fewer ROS events in W20–21 than in the following year before March (2 versus 3), they were by far more intense, with 44 and 106 mm of liquid precipitation each. These two events reduced the snow cover thickness and triggered winter snowmelt as shown in Fig. 3a–c–e and Fig. S3.1a. Based on these weather and snowpack

https://doi.org/10.5194/hess-2023-191
Preprint. Discussion started: 31 August 2023


Hydrology and Earth System Sciences
Discussions

conditions, we consider the winter 2020–21 to be representative of what could be expected for eastern Canada with global warming.

4.2 Earlier and slower melt

During the low-snow and warm winter, snowpack Q_{CC} was lower than in the reference winter. This is partly explained by a thinner snowpack with lower density (Fig. 3 and Fig. 10b–f–j). Warmer upper snow layers in W20–21 also contributed to the lower Q_{CC}. However, the lower snow layers were cooler in W20–21, which reduced the difference in Q_{CC} between the two years. Our observations are consistent with simulations by Jennings and Molotch (2020) for alpine and subalpine sites in the western US, where Q_{CC} is expected to decrease with increasing winter temperatures. Interestingly, the subcanopy snowpack had a larger Q_{CC} than in the forest gaps, despite being thinner and lighter. This would imply an enhanced outgoing heat flux under the canopy that would considerably cool down the snowpack compared to both gaps. However, as noted in section 3.2, this explanation would contradict the warmer snow surface under the canopy in both years (Figure 4). This behavior is expected as radiative cooling in forest is more likely to take place at locations of higher sky-view fraction, such as gaps. This suggests a cold bias in the monitored temperature profile time series under the canopy which lead to an overestimation of the cold content. Timelapse images taken at the canopy station indicate that the snowpack seemed to grow thicker under the ultrasonic sensor than at the thermistor array in both years, which could explain the discrepancy between Figure 3e–f and Figure 4.

Since the snowpack had a lower Q_{CC} in W20–21 in both the gaps and below the canopy, less energy was required to bring it to the melting point so snowmelt started earlier, consistent with what is expected in warmer winters (Barnett et al., 2005; López-Moreno et al., 2013; Guay et al., 2015; Jennings and Molotch, 2020). An earlier melt onset implied that net radiation was lower in W20–21, explaining a lower melt rate than in the reference winter (Fig. 5 and Fig. 6). When comparing the subcanopy snow to that found in the gaps, we observed a decrease in melt rate with canopy closure in both years, which is in agreement with previous studies as snowmelt is driven by $SWR_{net,bc}$ in forest gaps (Malle et al., 2019; Lawler and Link, 2011; Ellis et al., 2011). However, with less snow accumulating under the canopy due to interception, the snowpack melted-out earlier than in both gaps, in both years. Our results support conclusions from previous studies as canopy interception exerts the main control on snow accumulation patterns whereas distribution of shortwave radiation is the main driver of ablation patterns (Lundquist et al., 2013; Mazzotti et al., 2023; Dharmadasa et al., 2023). Overall, it shows that the structure of the canopy must be considered in models to precisely predict the effect of climate change on snow accumulation and melt dynamics in boreal forests.

4.3 Increased frozen soil under the canopy

A thinner snowpack allows more heat loss from the ground to the atmosphere, and as such, a larger ground heat flux (GHF; Fig. 7). A thinner snowpack in the low-snow winter thus led to a cooler soil than for the reference winter (Fig. 7; Table 5). This phenomenon was intensified under the canopy, where the snowpack was thinner and the GHF was larger. Our observations show that the heat loss was sufficient to favor soil freezing under the canopy, but not in the forest gaps. These

https://doi.org/10.5194/hess-2023-191
Preprint. Discussion started: 31 August 2023


Hydrology and Earth System Sciences
Discussions

findings are in partial agreement with Stadler et al. (1996), who observed a cooler ground under the canopy, where less snow accumulates. However, the authors also observed ground freezing in a nearby gap. This could be explained by the much lower snow accumulation at their study site compared to what was observed in the MF in both years.

Fig. 8 suggests that the soil has a similar pore space under the canopy and inside gaps, as it saturates at a volumetric water content (VWC) between 0.50 and 0.55 at all monitored sites. However, the seasonal low of VWC is at 0.38, 0.42 and 0.48 in the medium gap, the small gap and under the canopy, respectively, suggesting a higher water retention under the canopy and therefore smaller pores than in the gaps. This implies less potential for water content to increase in response to snowmelt or ROS event. The slower increase in VWC under the canopy at the onset of the 2021 snowmelt (Fig. 8a) also suggests that infiltration was limited, but not completely restricted compared to what was observed in the gaps. Based on previous experiments in the Montmorency Forest, Proulx and Stein (1997) concluded that ROS greater than 20 mm followed by a cold spell would cause macropores in the boreal soil to become ice-filled, limiting subsequent infiltration. According to this criterion, the two ROS of December 2020 (42 and 105 mm) should have favored the blockage of soil pores in W20–21. Overall, our results are in accordance with Demand et al. (2019), who observed a reduced infiltration into frozen soil compared with unfrozen but highly saturated soil during sprinkling experiments over a sandy loam in southern Germany.

4.4 Vertical temperature gradients and snow permeability

Our observations show that a thinner snowpack in W20–21 reduced load compaction and therefore limited snow densification, compared to W21–22. A thinner snowpack also led to higher vertical temperature gradients ($|\partial T/\partial z|$) in the low-snow and warm winter (Fig. 9), resulting in more pronounced faceting, lower SSA, and a higher permeability (K_s) than in W21–22 (Fig. 10). In terms of SSA, no significant difference was observed between the two years for the lowermost part of the snowpack, where we observed DH. This is because $|\partial T/\partial z|$ in both years was sufficient to favor DH development, and the SSA of DH remained always around 10 ± 2 m^2 kg^{-1}, regardless of its stage of development (Bouchard et al., 2022; Domine et al., 2018). In February and March, the $|\partial T/\partial z|$was larger in W20–21 than for the same period the next year. This resulted to a faster development of FC and DH and to a lower SSA in the middle part of the snowpack. Since snow permeability is closely related to snow metamorphism and $|\partial T/\partial z|$(Domine et al., 2013; Taillandier et al., 2007;Calonne et al., 2012), K_s shows a similar pattern to SSA in the snow profiles. When comparing the snowpack under the canopy to the one in both gaps, we observe that temperature gradient metamorphism was enhanced under the canopy, in line with observations from Bouchard et al. (2022). Interestingly, our field measurements in forest gaps and under a boreal canopy contradict Domine et al. (2007) who, based on general considerations, suggested a decrease in snow permeability with global warming mainly due to increased snow surface temperature. Our results suggest that if warmer winters lead to a large decrease in snowpack thickness, this could override the increase in surface temperature and lead to higher $|\partial T/\partial z|$ and permeability.

https://doi.org/10.5194/hess-2023-191
Preprint. Discussion started: 31 August 2023


Hydrology and Earth System Sciences
Discussions

4.5 Reduced spring streamflow

Figure 11 clearly shows that the spring freshet was earlier and reduced in the low-snow and warm winter compared to the reference winter. This suggests that an earlier and slower melt exerted a major influence on streamflow regime. Our results are consistent with the work of Musselman et al. (2017), who simulated reduced streamflow runoff with earlier and slower melt. However, this alone does not explain the large difference in spring runoff between the two years. As shown in Fig. 11, the precipitation for April and May was much lower in 2021 than in the following year (122 mm vs 253 mm). Given a temporal lag of 3 to 5 years between the recharge of the aquifer and groundwater outflow at BEREV-7A (Schilling et al., 2021), snowmelt and precipitation are likely the main contributors to spring streamflow. Overall, although enhanced soil freezing and a higher snowpack permeability in the low-snow year may have contributed to increase spring streamflow in 2021, our results show that a thin snowpack, combined to dry conditions that spring, significantly reduced the catchment hydrograph as compared to the reference year.

4.6 Limitations and shortcomings

In this study, we examined snow accumulation and melt dynamics from highly detailed in situ measurements to establish links between the various processes controlling spring streamflow in discontinuous boreal forest environments. Although this observational study combines snow accumulation and melt dynamics, soil freezing and snow microstructure in one unique dataset representative of the humid boreal forest, the analysis itself remains a case study. Other specific characteristics of the study site such as the slope, the aspect and the surrounding topography, influence the formation and the ablation of the snowpack in forested environments (Lundquist and Flint, 2006; Ellis et al., 2013; Mazzotti et al., 2023). To assess the impact of low-snow and warm winter conditions on snowpack dynamics at broad scales, the impact of these factors should be considered.

Some other shortcomings from this study may be relevant for future experimental research projects focusing on the impact of weather conditions on snowpack-related hydrological implications in discontinuous forest at the process scale. One experimental limitation to our study regards the spatial distribution of the soil monitoring. Soil moisture was only monitored at one depth in three nearby locations, which is insufficient to give insights on infiltration patterns at the catchment scale. It underscores the need of monitoring the soil VWC at multiple forest gaps and canopy locations in future studies to better understand soil infiltration dynamics in discontinuous boreal forests under a warming climate. Furthermore, a complete interpretation of soil liquid water content data would benefit from the knowledge of soil granulometry.

4.7 Climatic, hydrological and ecological implications

In the low-snow and warm winter, snowmelt started much earlier, but occurred over a longer period at all sites, resulting in an earlier melt-out compared to the reference winter. A shorter-lived snowpack in the boreal forest has climatic impacts, as the net shortwave radiation increases due to a reduction in surface albedo (Manninen and Stenberg, 2009) and contributes to a

https://doi.org/10.5194/hess-2023-191
Preprint. Discussion started: 31 August 2023


Hydrology and Earth System Sciences
Discussions

positive feedback loop that enhances global warming (Thackeray and Fletcher, 2015). Moreover, a decrease in snow cover extent in the boreal forest may increase the risk of summer hydrological drought due to a lower groundwater recharge (Van Loon et al., 2015). Based on the definition of Van Loon et al. (2015), the conditions in spring 2021 (Fig. 11) have the characteristics of a snowmelt drought.

With increasing warming-induced ROS events, the formation of melt-freeze layers, as we observed at the base of the W20–21 snowpack, and within the snowpack are likely to become more common. These could alter liquid water pathways, favoring water ponding and lateral flow over percolation (Eiriksson et al., 2013; Paquotte and Baraer, 2022; Webb et al., 2018). In addition to altering downward liquid water transport through the snowpack, melt-freeze formations can limit soil-atmosphere gas exchange, promoting hypoxic conditions in subnivean environments (Crawford and Braendle, 1996). Melt-freeze formations also limit access to food and movement of subnivean mammals (Johnsen et al., 2017; Poirier et al., 2019), and restrict foraging by large herbivores (Hansen et al., 2011; Schmelzer et al., 2020). As we observed in December 2020, intense ROS events also trigger winter snowmelt. This promotes low-snow conditions that can intensify soil freezing, as observed under the canopy snowpack in W20–21. Deeper soil freezing in forests decreases microbial activity and soil respiration in winter, thus reducing soil nitrogen recycling (Patel et al., 2018; Yang et al., 2019). In turn, this favors carbon accumulation which offsets increased soil respiration in summer (Patel et al., 2018). In summary, it seems clear that changes in snowpack thickness and structure with climate warming have both hydrological and ecological implications in the boreal forest.

5 Conclusion

Using dedicated field observations, we investigated the effects of a low-snow and warm winter on snow accumulation and melt dynamics, on soil thermal regime and moisture, and on snowpack physical properties under the canopy, and inside two forest gaps in a humid boreal site of eastern Canada. More precisely, we focused on winter 2020–21 (W20–21), which was exceptionally warm and dry, comparing it with a reference winter (W21-22), closer to climate normals. The experimental setup included snowpack and the soil thermal regime monitoring, along with monthly snow pit observations. Our results show that the snowpack was generally half as thick and started to melt earlier in the low-snow and warm winter, compared to the reference winter. This increased soil freezing under the canopy, but not in forest gaps, where the soil remained unfrozen, as for the reference winter. Although the snow surface was warmer in W20–21, the thinner snowpack led to an increase in the vertical temperature gradient, so kinetic growth was enhanced. This resulted in a higher snow permeability during the warm, low-snow year, particularly under the canopy. A thin and early melting snowpack, combined with less precipitation in spring, resulted in a much lower spring runoff in W20–21 than in the reference winter, suggesting that weather conditions were the main driver of spring freshet, rather than soil freezing and snowpack characteristics.

The conditions experienced in the winter 2020–21 at Montmorency Forest, such as warmer air, less snowfall, and a thinner snowpack, were exceptional compared to the past climatology, but may become the new norm in eastern Canada with climate change. Although this work is limited to a two-year comparison within a small catchment, it highlights the many potential effects, all together, of a changing climate on snow hydrology in a discontinuous boreal forest through a unique set of highly

detailed process-level observations. These are highly valuable for the snow science community as they will help improve existing modeling tools and develop new ones to address future challenges in snow hydrology.

Data availability. Data from snow pit measurements and from the monitoring stations in the medium and small gaps, and under the canopy are freely available at https://doi.org/10.5281/zenodo.8213204.

Author contributions. BB, DFN and FD designed the study. BB and ET collected and treated field data. BB conducted the analysis of the results with inputs from DFN, FD, FA, and TJ. BB wrote the manuscript, with feedbacks from all authors.

Competing interests. The authors declare that they have no conflict of interest.

Acknowledgements. The authors thank the staff of the Montmorency Forest for helping us logistically with field visits. We also thank Charles Villeneuve and Kino Leroux for preparing snowmobiles trails before our visits. The authors also thank Éric Boucher, Christian Juneau and Antoine Thiboult for helping in the deployment and the maintain of the monitoring stations. We thank Pierre-Erik Isabelle for providing radiation dataset. We finally thank all the people that accompanied Benjamin Bouchard and Etienne Tremblay on the field, especially the members of PÉGEAUX and the graduate students, post-doc, and research associates from the Hydrometeorology Lab at Laval University. The work of BB was founded by the Natural Sciences and Engineering Research Council (NSERC) and Sentinel North program. The authors acknowledge the financial contribution of Environment and Climate Change Canada through the Grants & Contributions program (projects #GCXE20M016 and #GCXE22M013) and the Cold-region climate projection for hydrological applications (EVAP-2; project #ALLRP 549108 – 19).

References

Albert, M., and Hardy, J.: Snowpack stratigraphy evolution at forested and open sites, in: Proceedings of the 50th Annual Eastern Snow Conference, Quebec City, Canada, 8-10 June 1993, 205-212, 1993.

Albert, M. R., and Perron, F. E.: Ice layer and surface crust permeability in a seasonal snow pack, Hydrol. Process., 14, 3207-3214, http://dx.doi.org/10.1002/1099-1085(20001230)14:18%3C3207::AID-HYP196%3E3.0.CO;2-C, 2000.

Barnett, T. P., Adam, J. C., and Lettenmaier, D. P.: Potential impacts of a warming climate on water availability in snow-dominated regions, Nature, 438, 303-309, http://dx.doi.org/10.1038/nature04141, 2005.

Barnhart, T. B., Molotch, N. P., Livneh, B., Harpold, A. A., Knowles, J. F., and Schneider, D.: Snowmelt rate dictates streamflow, Geophys. Res. Lett., 43, 8006-8016, http://dx.doi.org/10.1002/2016GL069690, 2016.

Berghuijs, W., Woods, R., and Hrachowitz, M.: A precipitation shift from snow towards rain leads to a decrease in streamflow, Nat. Clim. Change, 4, 583-586, http://dx.doi.org/10.1038/nclimate2246, 2014.

https://doi.org/10.5194/hess-2023-191
Preprint. Discussion started: 31 August 2023

Beven, K., and Germann, P.: Macropores and water flow in soils revisited, Water Resour. Res., 49, 3071-3092, http://dx.doi.org/10.1002/wrcr.20156, 2013.

Bouchard, B., Nadeau, D. F., and Domine, F.: Comparison of snowpack structure in gaps and under the canopy in a humid boreal forest, Hydrol. Process., 36, http://dx.doi.org/10.1002/hyp.14681, 2022.

Bründl, M., Schneebeli, M., and Flühler, H.: Routing of canopy drip in the snowpack below a spruce crown, Hydrol. Process., 13, 49-58, http://dx.doi.org/10.1002/(SICI)1099-1085(199901)13:1%3C49::AID-HYP700%3E3.0.CO;2-L, 1999.

Calonne, N., Geindreau, C., Flin, F., Morin, S., Lesaffre, B., Rolland du Roscoat, S., and Charrier, P.: 3-D image-based numerical computations of snow permeability: links to specific surface area, density, and microstructural anisotropy, Cryosphere, 6, 939-951, https://doi.org/10.5194/tc-6-939-2012, 2012.

Choquette, Y., Ducharme, P., and Rogoza, J.: CS725, an accurate sensor for the snow water equivalent and soil moisture measurements, in: Proceedings of the International Snow Science Workshop, Grenoble, France, 7-11 October 2013, 931-936, 2013.

Colbeck, S. C.: Theory of metamorphism of dry snow, Journal of Geophysical Research: Oceans, 88, 5475-5482, https://doi.org/10.1029/jc088ic09p05475, 1983.

Conger, S. M., and McClung, D. M.: Comparison of density cutters for snow profile observations, J. Glaciol., 55, 163-169, http://dx.doi.org/10.3189/002214309788609038, 2009.

Crawford, R. M. M., and Braendle, R.: Oxygen deprivation stress in a changing environment, J. Exp. Bot, 47, 145-159, http://dx.doi.org/10.1093/jxb/47.2.145, 1996.

Demand, D., Selker, J. S., and Weiler, M.: Influences of macropores on infiltration into seasonally frozen soil, Vadose Zone J., 18, 1-14, https://dx.doi.org/10.2136/vzj2018.08.0147, 2019.

Dharmadasa, V., Kinnard, C., and Baraër, M.: Topographic and vegetation controls of the spatial distribution of snow depth in agro-forested environments by UAV lidar, Cryosphere, 17, 1225-1246, https://dx.doi.org/10.5194/tc-17-1225-2023, 2023.

Domine, F., Taillandier, A., Houdier, S., Parrenin, F., Simpson, W. R., and Douglas, T. A.: Interactions between snow metamorphism and climate: Physical and chemical aspects, in: Physics and Chemistry of Ice, edited by: Kuhs, W. F., Royal Society of Chemistry, Cambridge, UK, 27-46, 2007.

Domine, F., Barrere, M., Sarrazin, D., Morin, S., and Arnaud, L.: Automatic monitoring of the effective thermal conductivity of snow in a low-Arctic shrub tundra, Cryosphere, 3, 1265-1276, http://dx.doi.org/10.5194/tc-9-1265-2015, 2015.

Domine, F., Belke-Brea, M., Barrere, M., Sarrazin, D., Poirier, M., and Arnaud, L.: Soil moisture, wind speed and depth hoar formation in the Arctic snowpack, J. Glaciol., 64, 990-1002, https://dx.doi.org/10.1017/jog.2018.89, 2018.

Ellis, C. R., Pomeroy, J. W., Essery, R. L. H., and Link, T. E.: Effects of needleleaf forest cover on radiation and snowmelt dynamics in the Canadian Rocky Mountains, Can. J. Forest Res., 41, 608-620, http://dx.doi.org/10.1139/X10-227, 2011.

https://doi.org/10.5194/hess-2023-191
Preprint. Discussion started: 31 August 2023

Ellis, C. R., Pomeroy, J. W., and Link, T. E.: Modeling increases in snowmelt yield and desynchronization resulting from forest gap-thinning treatments in a northern mountain headwater basin, Water Resour. Res., 49, 936-949, http://dx.doi.org/10.1002/wrcr.20089, 2013.

Fourteau, K., Domine, F., and Hagenmuller, P.: Impact of water vapor diffusion and latent heat on the effective thermal conductivity of snow, Cryosphere, 15, 2739-2755, https://doi.org/10.5194/tc-15-2739-2021, 2021.

Furey, P. R., Kampf, S. K., Lanini, J. S., and Dozier, A. Q.: A stochastic conceptual modeling approach for examining the effects of climate change on streamflows in mountain basins, J. Hydrometeorol., 13, 837-855, http://dx.doi.org/10.1175/JHM-D-11-037.1, 2012.

Fuss, C. B., Driscoll, C. T., Green, M. B., and Groffman, P. M.: Hydrologic flowpaths during snowmelt in forested headwater catchments under differing winter climatic and soil frost regimes, Hydrol. Process., 30, 4617-4632, http://dx.doi.org/10.1002/hyp.10956, 2016.

Gallet, J.-C., Domine, F., Zender, C. S., and Picard, G.: Measurement of the specific surface area of snow using infrared reflectance in an integrating sphere at 1310 and 1550 nm, Cryosphere, 3, 167-182, http://dx.doi.org/10.5194/tc-3-167-2009, 2009.

Goodrich, L. E.: The influence of snow cover on the ground thermal regime, Can. Geotech. J., 19, 421-432, http://dx.doi.org/10.1139/t82-047, 1982.

Granger, R. J., Gray, D. M., and Dyck, G. E.: Snowmelt infiltration to frozen Prairie soils, Can. J. Earth Sci., 21, 669-677, http://dx.doi.org/10.1139/e84-073, 1984.

Grenfell, T. C., and Warren, S. G.: Representation of a nonspherical ice particle by a collection of independent spheres for scattering and absorption of radiation, J. Geophys. Res., 104, 31697-31709, http://dx.doi.org/10.1029/1999JD900496, 1999.

Guay, C., Minville, M., and Braun, M.: A global portrait of hydrological changes at the 2050 horizon for the province of Québec, Canadian Water Resources Journal/Revue canadienne des ressources hydriques, 40, 285-302, http://dx.doi.org/10.1080/07011784.2015.1043583, 2015.

Guillemette, F., Plamondon, A. P., Prévost, M., and Lévesque, D.: Rainfall generated stormflow response to clearcutting a boreal forest: peak flow comparison with 50 world-wide basin studies, J. Hydrol., 302, 137-153, http://dx.doi.org/10.1016/j.jhydrol.2004.06.043, 2005.

Hamlet, A. F., Mote, P. W., Clark, M. P., and Lettenmaier, D. P.: Effects of temperature and precipitation variability on snowpack trends in the Western United States, J. Climate, 18, 4545-4561, http://dx.doi.org/10.1175/JCLI3538.1, 2005.

Hansen, B. B., Aanes, R., Herfindal, I., Kohler, J., and Sæther, B.-E.: Climate, icing, and wild arctic reindeer: past relationships and future prospects, Ecology, 92, 1917-1923, http://dx.doi.org/10.1890/11-0095.1, 2011.

https://doi.org/10.5194/hess-2023-191
Preprint. Discussion started: 31 August 2023

Hardy, J. P., Melloh, R., Robinson, P., and Jordan, R.: Incorporating effects of forest litter in a snow process model, Hydrol. Process., 14, 3227-3237, http://dx.doi.org/10.1002/1099-1085(20001230)14:18%3C3227::AID-HYP198%3E3.0.CO;2-4, 2000.

Hardy, J. P., Groffman, P. M., Fitzhugh, R. D., Henry, K. S., Welman, A. T., Demers, J. D., Fahey, T. J., Driscoll, C. T., Tierney, G. L., and Nolan, S.: Snow depth manipulation and its influence on soil frost and water dynamics in a northern hardwood forest, Biogeochemistry, 56, 151-174, http://dx.doi.org/10.1023/A:1013036803050, 2001.

Il Jeong, D., and Sushama, L.: Rain-on-snow events over North America based on two Canadian regional climate models, Clim. Dynam., 50, 303-316, http://dx.doi.org/10.1007/s00382-017-3609-x, 2018.

IPCC: Climate Change 2022: Impacts, Adaptation, and Vulnerability. Contribution of Working Group II to the Sixth Assessment Report of the Intergovernmental Panel on Climate Change, Cambridge, UK, 2022.

Ireson, A. M., Barr, A. G., Johnstone, J. F., Mamet, S. D., van der Kamp, G., Whitfield, C. J., Michel, N. L., North, R. L., Westbrook, C. J., DeBeer, C., Chun, K. P., Nazemi, A., and Sagin, J.: The changing water cycle: the Boreal Plains ecozone of Western Canada, WIREs Water, 2, 505-521, http://dx.doi.org/10.1002/wat2.1098, 2015.

Jennings, K. S., and Molotch, N. P.: Snowfall fraction, cold content, and energy balance changes drive differential response to simulated warming in an alpine and subalpine snowpack, Front. Earth Sci., 8, http://dx.doi.org/10.3389/feart.2020.00186, 2020.

Jonas, T., Webster, C., Mazzotti, G., and Malle, J.: HPEval: A canopy shortwave radiation transmission model using high-resolution hemispherical images, Agric. For. Meteorol., 284, 107903, http://dx.doi.org/10.1016/j.agrformet.2020.107903, 2020.

Jones, H., and Pomeroy, J.: Early spring snowmelt in a small boreal forest watershed: influence of concrete frost on the hydrology and chemical composition of streamwaters during rain-on-snow events, in: Proceedings of the Eastern Snow Conference, 17-19 May 2001, 209-218, 2001.

Kane, D. L., and Stein, J.: Water movement into seasonally frozen soils, Water Resour. Res., 19, 1547-1557, http://dx.doi.org/10.1029/WR019i006p01547, 1983.

Kunkel, K. E., Robinson, D. A., Champion, S., Yin, X., Estilow, T., and Frankson, R. M.: Trends and extremes in Northern Hemisphere snow characteristics, Current Climate Change Reports, 2, 65-73, https://dx.doi.org/10.1007/s40641-016-0036-8, 2016.

Lackner, G., Domine, F., Nadeau, D. F., Parent, A.-C., Anctil, F., Lafaysse, M., and Dumont, M.: On the energy budget of a low-Arctic snowpack, Cryosphere, 16, 127-142, http://dx.doi.org/10.5194/tc-16-127-2022, 2022.

Laternser, M., and Schneebeli, M.: Long-term snow climate trends of the Swiss Alps (1931-99), Int. J. Climatol., 23, 733-750, http://dx.doi.org/10.1002/joc.912, 2003.

Lawler, R. R., and Link, T. E.: Quantification of incoming all-wave radiation in discontinuous forest canopies with application to snowmelt prediction, Hydrol. Process., 25, 3322-3331, http://dx.doi.org/10.1002/hyp.8150, 2011.

https://doi.org/10.5194/hess-2023-191
Preprint. Discussion started: 31 August 2023

López-Moreno, J. I., Pomeroy, J. W., Revuelto, J., and Vicente-Serrano, S. M.: Response of snow processes to climate change: spatial variability in a small basin in the Spanish Pyrenees, Hydrol. Process., 27, 2637-2650, https://dx.doi.org/10.1002/hyp.9408, 2013.

Luce, C. H., and Holden, Z. A.: Declining annual streamflow distributions in the Pacific Northwest United States, 1948-2006, Geophys. Res. Lett., 36, L16401, http://dx.doi.org/10.1029/2009GL039407, 2009.

Lundquist, J. D., and Flint, A. L.: Onset of snowmelt and streamflow in 2004 in the Western United States: How shading may affect spring streamflow timing in a warmer world, J. Hydrometeorol., 7, 1199-1217, http://dx.doi.org/10.1175/JHM539.1, 2006.

Lundquist, J. D., Dickerson-Lange, S. E., Lutz, J. A., and Cristea, N. C.: Lower forest density enhances snow retention in regions with warmer winters: A global framework developed from plot-scale observations and modeling, Water Resour. Res., 49, 6356-6370, http://dx.doi.org/10.1002/wrcr.20504, 2013.

Malle, J., Rutter, N., Mazzotti, G., and Jonas, T.: Shading by trees and fractional snow cover control the subcanopy radiation budget, J. Geophys. Res.-Atmos., 124, 3195-3207, http://dx.doi.org/10.1029/2018JD029908, 2019.

Manninen, T., and Stenberg, P.: Simulation of the effect of snow covered forest floor on the total forest albedo, Agric. For. Meteorol., 149, 303-319, http://dx.doi.org/10.1016/j.agrformet.2008.08.016, 2009.

Mazzotti, G., Currier, W. R., Deems, J. S., Pflug, J. M., Lundquist, J. D., and Jonas, T.: Revisiting snow cover variability and canopy structure within forest stands: Insights from airborne LiDAR data, Water Resour. Res., 55, 6198-6216, http://dx.doi.org/10.1029/2019WR024898, 2019.

Mazzotti, G., Webster, C., Quéno, L., Cluzet, B., and Jonas, T.: Canopy structure, topography, and weather are equally important drivers of small-scale snow cover dynamics in sub-alpine forests, Hydrol. Earth Syst. Sc., 27, 2099-2121, https://dx.doi.org/10.5194/hess-27-2099-2023, 2023.

Melloh, R. A., Hardy, J. P., Davis, R. E., and Robinson, P. B.: Spectral albedo/reflectance of littered forest snow during the melt season, Hydrol. Process., 15, 3409-3422, http://dx.doi.org/10.1002/hyp.1043, 2001.

Mohammed, A. A., Kurylyk, B. L., Cey, E. E., and Hayashi, M.: Snowmelt infiltration and macropore flow in frozen soils: Overview, knowledge gaps, and a conceptual framework, Vadose Zone J., 17, 1-15, http://dx.doi.org/10.2136/vzj2018.04.0084, 2018.

Molotch, N. P., Barnard, D. M., Burns, S. P., and Painter, T. H.: Measuring spatiotemporal variation in snow optical grain size under a subalpine forest canopy using contact spectroscopy, Water Resour. Res., 52, 7513-7522, http://dx.doi.org/10.1002/2016WR018954, 2016.

Morin, S., Domine, F., Arnaud, L., and Picard, G.: In-situ monitoring of the time evolution of the effective thermal conductivity of snow, Cold Reg. Sci. Technol., 64, 73-80, http://dx.doi.org/10.1016/j.coldregions.2010.02.008, 2010.

Musselman, K. N., Clark, M. P., Liu, C., Ikeda, K., and Rasmussen, R.: Slower snowmelt in a warmer world, Nat. Clim. Change, 7, 214-219, http://dx.doi.org/10.1038/nclimate3225, 2017.

Ouranos, and MELCCFP: Guide de l'atlas hydroclimatique du Québec méridional, Quebec City, Can, 2022.

https://doi.org/10.5194/hess-2023-191
Preprint. Discussion started: 31 August 2023

690 Patel, K. F., Tarariw, C., MacRae, J. D., Ohno, T., Nelson, S. J., and Fernandez, I. J.: Soil carbon and nitrogen responses to snow removal and concrete frost in a northern coniferous forest, Can. J. Soil Sci., 98, 436-447, http://dx.doi.org/10.1139/cjss-2017-0132, 2018.

Pepin, N., Bradley, R. S., Diaz, H., Baraër, M., Caceres, E., Forsythe, N., Fowler, H., Greenwood, G., Hashmi, M., and Liu, X.: Elevation-dependent warming in mountain regions of the world, Nat. Clim. Change, 5, 424-430,
695 https://dx.doi.org/10.1038/nclimate2563, 2015.

Pierre, A., Jutras, S., Smith, C., Kochendorfer, J., Fortin, V., and Anctil, F.: Evaluation of catch efficiency transfer functions for unshielded and single-alter-shielded solid precipitation measurements, J. Atmos. Ocean Tech., 36, 865-881, https://dx.doi.org/10.1175/JTECH-D-18-0112.1, 2019.

Pomeroy, J. W., Parviainen, J., Hedstrom, N., and Gray, D. M.: Coupled modelling of forest snow interception and sublimation,
700 Hydrol. Process., 12, 2317-2337, http://dx.doi.org/10.1002/(SICI)1099-1085(199812)12:15%3C2317::AID-HYP799%3E3.0.CO;2-X, 1998.

Price, D. T., R.I., A., Brown, K. J., Flannigan, M. D., Fleming, R. A., Hogg, E. H., Girardin, M. P., Lakusta, T., Johnston, M., McKenney, D. W., Pedlar, J. H., Stratton, T., Sturrock, R. N., Thompson, I. D., Trofymow, J. A., and Venier, L. A.: Anticipating the consequences of climate change for Canada's boreal forest ecosystems, Environ. Rev., 21, 322-365,
705 http://dx.doi.org/10.1139/er-2013-0042, 2013.

Proulx, S., and Stein, J.: Classification of meteorological conditions to assess the potential for concrete frost formation in boreal forest floors, Can. J. Forest Res., 27, 953-958, http://dx.doi.org/10.1139/x96-217, 1997.

Scheffer, M., Hirota, M., Holmgren, M., Van Nes, E. H., and Chapin, F. S.: Thresholds for boreal biome transitions, P. Natl. Acad. Sci. USA, 109, 21384-21389, http://dx.doi.org/10.1073/pnas.1219844110, 2012.

710 Schilling, O. S., Parajuli, A., Müller, T. U., Tremblay, Y., Brennwald, M. S., Nadeau, D. F., Jutras, S., Kipfer, R., and Therrien, R.: Quantifying groundwater recharge dynamics and unsaturated zone processes in snow-dominated catchments via on-site dissolved gas analysis, Water Resour. Res., 57, https://dx.doi.org/10.1029/2020WR028479, 2021.

Schmelzer, I., Lewis, K. P., Jacobs, J. D., and McCarthy, S. C.: Boreal caribou survival in a warming climate, Labrador, Canada 1996-2014, Glob. Ecol. Conser., 23, e010308, http://dx.doi.org/10.1016/j.gecco.2020.e01038, 2020.

715 Shanley, J. B., and Chalmers, A.: The effect of frozen soil on snowmelt runoff at Sleepers River, Vermont, Hydrol. Process., 13, 1843-1857, http://dx.doi.org/10.1002/(SICI)1099-1085(199909)13:12/13%3C1843::AID-HYP879%3E3.0.CO;2-G, 1999.

Shook, K., and Pomeroy, J.: Changes in the hydrological character of rainfall on the Canadian prairies, Hydrol. Process., 26, 1752-1766, http://dx.doi.org/10.1002/hyp.9383, 2012.

720 Sicart, J. E., Pomeroy, J. W., Essery, R. L. H., and Bewley, D.: Incoming longwave radiation to melting snow: observations, sensitivity and estimation in Northern environments, Hydrol. Process., 20, 3697-3708, http://dx.doi.org/10.1002/hyp.6383, 2006.

https://doi.org/10.5194/hess-2023-191
Preprint. Discussion started: 31 August 2023

Stadler, D., Wunderli, H., Auckenthaler, A., Flühler, H., and Bründl, M.: Measurement of frost-induced snowmelt runoff in a forest soil, Hydrol. Process., 10, 1293-1304, http://dx.doi.org/10.1002/(SICI)1099-1085(199610)10:10%3C1293::AID-HYP461%3E3.0.CO;2-I, 1996.

Stähli, M., Jansson, P.-E., and Lundin, L.-C.: Preferential water flow in a frozen soil - A two-domain model approach, Hydrol. Process., 10, 1305-1316, http://dx.doi.org/10.1002/(SICI)1099-1085(199610)10:10%3C1305::AID-HYP462%3E3.0.CO;2-F, 1996.

Sun, N., Wigmosta, M., Zhou, T., Lundquist, J., Dickerson-Lange, S., and Cristea, N.: Evaluating the functionality and streamflow impacts of explicitly modelling forest-snow interactions and canopy gaps in a distributed hydrologic model, Hydrol. Process., 32, http://dx.doi.org/10.1002/hyp.13150, 2018.

Teich, M., Giunta, A. D., Hagenmuller, P., Bebi, P., Schneebeli, M., and Jenkins, M. J.: Effects of bark beetle attacks on forest snowpack and avalanche formation - Implications for protection forest management, Forest Ecol. Manag., 438, 186-203, http://dx.doi.org/10.1016/j.foreco.2019.01.052, 2019.

Thackeray, C. W., and Fletcher, C. G.: Snow albedo feedback: Current knowledge, importance, outstanding issues and future directions, Prog. Phys. Geog., 40, 392-408, http://dx.doi.org/10.1177/0309133315620999, 2015.

Valencia Giraldo, M. d. C., Ricard, S., and Anctil, F.: Assessment of the Potential Hydrological Impacts of Climate Change in Quebec—Canada, a Refined Neutral Approach, Water-Sui, 15, 584, http://dx.doi.org/10.3390/w15030584, 2023.

Van Loon, A. F., Ploum, S. W., Parajka, J., Fleig, A. K., Garnier, E., Laaha, G., and Van Lanen, H. A. J.: Hydrological drought types in cold climates: quantitative analysis of causing factors and qualitative survey of impacts, Hydrol. Earth Syst. Sc., 4, 1993-2016, http://dx.doi.org/10.5194/hess-19-1993-2015, 2015.

Vincent, L. A., and Mekis, E.: Changes in daily and extreme temperature and precipitation indices for Canada over the twentieth century, Atmos.-Ocean, 44, 177-193, http://dx.doi.org/10.3137/ao.440205, 2006.

Watanabe, K., and Kugisaki, Y.: Effect of macropores on soil freezing and thawing with infiltration, Hydrol. Process., 31, 270-278, http://dx.doi.org/10.1002/hyp.10939, 2017.

Xu, C. Y., and Halldin, S.: The Effect of Climate Change on River Flow and Snow Cover in the NOPEX Area Simulated by a Simple Water Balance Model, Nord. Hydrol., 28, 273-282, 1997.

Yang, K., Peng, C., Peñuelas, J., Kardol, P., Li, Z., Zhang, L., Ni, X., Yue, K., Tan, B., Yin, R., and Xu, Z.: Immediate and carry-over effects of increased soil frost on soil respiration and microbial activity in a spruce forest, Soil Biol. Biochem., 135, 51-59, http://dx.doi.org/10.1016/j.soilbio.2019.04.012, 2019.

Zhang, T.: Influence of the seasonal snow cover on the ground thermal regime: An overview, Rev. Geophys., 43, http://dx.doi.org/10.1029/2004RG000157, 2005.

Zheng, B., Ciais, P., Chevallier, F., Yang, H., Canadell, J. G., Chen, Y., van der Velde, I. R., Aben, I., Chuvieco, E., Davis, S. J., Deeter, M., Hong, C., Kong, Y., Li, H., Li, H., Lin, X., He, K., and Zhang, Q.: Record-high CO2 emissions from boreal fires in 2021, Science, 379, 912-917, http://dx.doi.org/10.1126/science.ade0805, 2023.